Microburner for Wobbe Index measurements

Egbert Mekenkamp
Exam commitee: *Prof. dr. ir. J.C. Lötters, Prof. dr. J.C.T. Eijkel, Dr. ir. R.J. Wiegerink, Ir. D. Alveringh*

***Abstract*—A Wobbe Index by combustions is able to measure the exchangeability of different gasses. In this report the size of a Wobbe Index Meter is scaled to micrometer-dimensions. To do so, multiple physical aspects are taken into account such as temperature, fluid flows, mechanical expansion due to heat and combustion effects. To limit the influence of each different physical property, the problem is divided into 3 almost independent parts, namely mixing, preheating and combustion. This leads to eleven designs where the difference is emphasized on the combustion section. The devices are fabricated using the Surface Channel technology (SCT) process. During the process multiple chips were unusable resulting that not every design can be measured. The TCR of the resistors shows a high correlation on chip with a maximum variation of <4.8%. by applying gas and heating the heaters a temperature increase of 70°C could be observed. No temperature variation due to fluid flow could be observed thus no temperature of the gas could be measured.**

I. Introduction

A Wobbe Index meter measures the caloric value of a fuel gas via the heat produced by burning gas at standard temperature and pressure(stp, 293 K and 1 atmosphere). The output is the Wobbe Index named after engineer and mathematician Goffredo Wobbe. It is a measure for the interchangeability of fuel gas; gasses with the same Wobbe index will release the same energy output. The definition of the Wobbe Index(WI) is:

$$WI = \frac{H}{\sqrt{G_s}} \tag{1}$$

where H [J/m^3] is the higher caloric value and G_s [-] the specific gravity of the gas.

In the last 50 years, there have been only moderate evolutions with respect to novel techniques, compact design and cost reduction. At the moment an accurate estimate of the Wobbe index can only be obtained with conventional large and expensive equipment such as a Wobbe index meter[1] or a gas chromatograph[2].

To combine the Wobbe Index Meter with an already existing micro-Coriolis technology a adjusted combustion with an open flame since it is easy to integrate within the technology and a direct relation between the combustion energy and the measured temperature can be obtained[3]. The measurements will be preformed using a continuous flame and the energy balance at the end of the chip will be a measure for the combustion energy and the thermal losses.

In the next section the basic structure and operating principle is explained. To have the chip operating correctly certain theory is needed which is given in the section Theory. In the section Designs the designs are made using the theory. Then fabrication is explained in section Fabrication process and problems after fabrication are discussed. After fabrication the working chips are tested and the measurement set-ups and results are given in section Results.

II. Basic structure and Operating Principle

In Figure 1,a schematic diagram of the envisioned Wobbe index meter [4] is shown. The complete system can be integrated on a silicon chip with dimensions in the order of 1.5cm x 1.5cm. At the gas and air inlets it has micro Coriolis mass flow meters [5] that measure both the mass flow and density. Next, the fuel gas and air are pre-heated up to a temperature of about 600 °C in separate channels. Integrated silicon nitride channels are used, which can withstand temperatures up to approximately 1000 °C, which is the deposition temperature of silicon nitride. On a thermally insulated part of the chip, the gas and air are mixed in a reaction chamber and the elevated temperature is sufficient for spontaneous combustion of the gas.

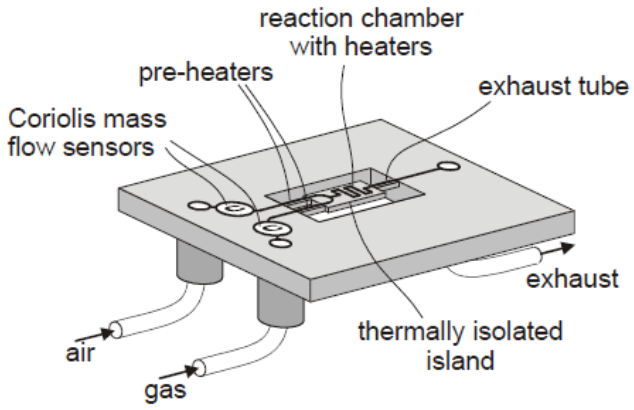

Fig. 1. Schematic design of the envisioned on-chip energy content measurement system

During spontaneous combustion, the produced heat will result in a further elevation of temperature, which is a measure for the energy content of the gas. A careful design is needed such that the maximum temperature for the silicon nitride channels is not exceeded. Optionally, a catalyst may be introduced in the reaction chamber, which significantly complicates the fabrication process, but also lowers the temperature needed for spontaneous burning to about 300 °C.

The schematic view initial design of the integrated Wobbe Index Meter is shown in Figure 2. The system consists of 2 gas inlets, a mixer, heaters, combustion chamber and an exhaust outlet. In must be noted that the micro Coriolis mass flow meter have not been incorporated in this initial design.

At ambient temperature the fuel gas and air flow are controlled by flow mass meters and flow into the chip. Next,

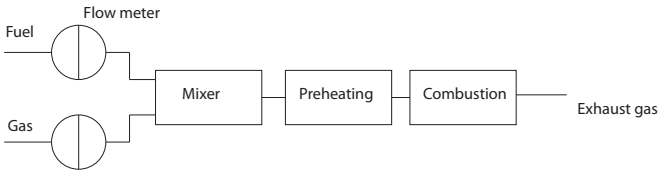

Fig. 2. schematic initial design of the integrated Wobbe Index Meter

the gas and air are mixed and heated up to just below the ignition point. Next, in the combustion chamber the gas is combusted resulting in a elevation in temperature which can be measured by resistive temperature sensors. The temperature elevation will be a measure of the heat generated by the combustion of the fuel gas.

III. Theory

Since the integrated Wobbe Index Meter is a multidisciplinary problem, in this section the most important aspects of each discipline will be discussed. There will be therefore a section on fluidics, combustion, mixing, suspension and thermodynamics. For each discipline the relevant theory will be given.

A. Fluidics

The fluid properties of gas influence the dynamics of the design. Therefore several aspects of a fluid flow are taken into account, to start with the basic kinetics, the flow and pressure and mixing that occurs due to heterogeneous flow.

1) Gas kinetics: The behaviour of ideal gas can be explained using the ideal gas law which is:

$$pV = nRT \tag{2}$$

where p [Pa] is the pressure, V [m^3] is the volume of the chamber, n [-] is the amount of mole, R [J/(mol K)] si the gas constant and T [K] is the temperature. The ideal gas law is an approximation of the behaviour of the gas since the interaction between molecules and the volume of the molecules is neglected.

2) Flow and pressure: Since some applications work at low pressures, the pressure drop is also limited. The pressure drop ΔP [Pa] can be calculated using the hydraulic resistance described by the Hagen-Poiseuille equation and the flow through the pipe[6]:

$$\Delta P = 128\mu \frac{L\phi_V}{\pi D^4} \ [Pa] \tag{3}$$

where L [m] is the length of the tube, μ [m^2/s] is the dynamic viscosity of the fluid, ϕ_V [m^3/s] is the volume flow rate and D [m]is the diameter of the tube. Since the Hagen-Poiseuille equation is only valid for laminar flow, the Reynolds number needs to be calculated. A Reynolds number below 2300 describes a laminar flow, a higher number indicates that the flow will be turbulent. The Reynolds number [-] in a cylindrical tube is given by:

$$Re = \frac{\rho \overrightarrow{v} D_h}{\mu} \tag{4}$$

where ρ [kg/m^3]is the density of the fluid, v [m/s] the mean velocity of the object relative to the fluid and D_h [m] is the hydraulic diameter. The hydraulic diameter is defined as:

$$D_h = \frac{4A}{P} \tag{5}$$

where A [m^2] is the cross-sectional area of the tube and P [m] the perimeter of the tube.

3) Mixing: To obtain complete combustion it is desired to have a nicely fuel-air mixture. Therefore the gases needs to be mixed. Familiar examples are pumping and stirring. Since the mixing happens on chip the mixing must be able to be integrated to the chip. It is also known that the gas exists of a laminar flow. It is therefore difficult to pump and to stir. Therefore mixing by means of diffusion investigated. This diffusion can be altered by increasing the contact area between the two (or more) different compounds. Since the width of each layer decreases, the time needed for fully diffusion also decreases. The standard diffusion equation is given in equation 6[7].

$$\frac{\partial c}{\partial t} = D\frac{\partial^2 c}{\partial x^2} \tag{6}$$

For a methane-air mixture the diffusion constant is $D = 2 \cdot 10^{-5} m^2/s$[8]. To satisfy the differential equation boundary values are required. The boundary conditions applying to the system used is that no atoms are lost in the system and no atoms are added to the system, thus in this case the following Neumann boundary conditions will be applied:

$$\left.\frac{\partial c}{\partial x}\right|_{x=0} = \left.\frac{\partial c}{\partial x}\right|_{x=L} = 0 \tag{7}$$

B. Combustion

The device could be used for multiple applications, but since it will be used to measure the Wobbe Index of natural gas, the main reaction is based on methane. The chemical equation balance and released energy of methane is:

$$CH_4(g) + 2\ O_2(g) \rightarrow CO_2(g) + 2\ H_2O(g) \tag{8}$$

$$CH_4 \rightarrow C + 2\ H_2 \quad [74.81kJ/mole] \tag{9}$$

$$C + O_2 \rightarrow CO_2 \quad [-393.51kJ/mole] \tag{10}$$

$$2\ H_2 + O_2 \rightarrow 2\ H_2O \quad [-483.63kJ/mole] \tag{11}$$

This leads to a total energy release of:

$$\Delta H_f = -802.33kJ/mole \tag{12}$$

It must be noted this chemical reaction is only first order reaction and explaining the combustion in an understandable manner. In reality a much more profound combustion chain is composed. This is increased when air is used instead of oxygen. To simplify the matter, the composition of air used is 21% oxygen and 79% nitrogen. This means the equation is altered into:

$$CH_4(g) + 2\frac{1}{0.2094}Air(g) \tag{13}$$
$$= CH_4(g) + 2\ O_2(g) + 9.52\ N_2(g) \tag{14}$$
$$\rightarrow CO_2(g) + 2\ H_2O(g) + 9.52\ N_2(g) \tag{15}$$

Thus for one mole oxygen gas, 4.76 mole of Air is needed.

1) Combustion velocity: The combustion velocity is approximated by a speed of 37 cm/s[9] when the applied gas is at 293 K. Since the temperature is first elevated to slightly below its critical value the burning velocity will rise, as less heat is needed to heat the unburned gas. The velocity is altered to[10]:

$$S_L = S_{L0}\left(\frac{T}{T_0}\right)^{\alpha} \tag{16}$$

where S_L [m/s] is the burning velocity and T [K] the temperature. Subscript 0 denotes the reference value. The value α differs for each gas composition, for stoichiometric methane-air this value is 1.58. This leads to a combustion velocity of 1.8 m/s.

2) Ignition composition: To sustain the flame there are some limitations that needs to be met. The composition of the gas limits the flammability of the gas. The gas can still combust at when lower amounts of fuel is applied, up to a limit of 5 volume percent[11]. In this case there is an excess of oxygen but all methane is burned. The upper flammable limit of methane-air is 15 volume percent[11]. In this case there is an excess of methane. This means not all methane is burned, which is undesired for the measurement, since no relation between the temperature and amount of combusted methane can be achieved.

Another limitation is the flame stabilization. There are two main types of instabilities that can occur to the flame, which are Flashback and Blowoff. Flashback occurs when the burning velocity is larger than the flow velocity through the tube. The gas will move backwards inside the tube and eventually it will kill the flame. The other instability occurs when the burning velocity is smaller than the flow velocity. In this case the flame will travel through the tube towards the end and the flame will exit the tube extinguish. This means there must be inside the chip a position on which the flame can stabilize.

3) Ignition temperature: The combustion temperature of methane can be calculated to be at least 810 K[12] at 1 bar. In experiments this temperature tends to be much higher than the theoretical value and normal combustion temperatures for methane are around 873 K[13].

4) Water vapour: During the combustion also water vapour is created. This vapour is a fraction of about 20% of the output pressure:

$$\frac{2H_2O}{2H_2O + 3.76N_2 + 1CO_2} = \frac{2}{10} \tag{17}$$

This means the pressure of water is 20 kPa in case a pressure of 1 atmosphere is used and this water pressure corresponds to liquefaction at 333 K. This means the temperature needs to stay about this threshold to prevent condensation of water inside the tube.

C. Thermodynamics

Heat is moving along objects and is transfered between objects. How it is moving can be categorized into three groups, namely conduction, convection and radiation. Heat transferring by conduction is noticed in metals, hereby the heat is moving rapidly within objects. Convection occurs when a fluid or gas is moving along a hot object. Radiation is the transfer of heat to a non-moving fluid or gas by means of electromagnetic radiation. This is also shown in Figure 3.

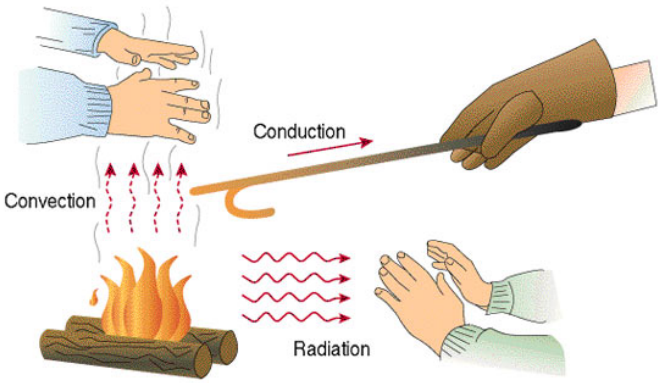

Fig. 3. Figure showing the three ways of heat transfer[14]

For each type of thermodynamics a corresponding equation can be used:

$$\textbf{Conduction:} Q = \frac{kA}{x}(T - T_0) \tag{18}$$
$$\textbf{Convection:} Q = hA(T - T_0) \tag{19}$$
$$\textbf{Radiation:} Q = \epsilon\sigma A(T^4 - T_0^4) \tag{20}$$

where k [W/mK] is thermal coefficient, h [W/m^{2}K] the heat transfer coefficient, A [m^2] the surface area, x [m] the length, ϵ [-] the emissivity, σ [J/(sm^{2}K^4)] the Stephan-Boltzmann constant and T [K] the temperature. Since the dimensions are quite small, within the micrometer range, a better approximation is done by using the advection-diffusion equation. In this equation both the diffusion, that is the microdynamic behaviour of conduction and advection, which is transferring energy due to fluid flow are included. The advection-diffusion equation is given as:

$$0 = \nabla \cdot (\alpha \nabla T) - \nabla \cdot (vT) \tag{21}$$

This is in case of a stationary result. T is the temperature and α [m^2/s] is the thermal diffusion constant and v [m/s] is the flow velocity. The conventional manner to calculate the temperature is by means of the added energy related to the heat capacity of the material:

$$\frac{dT}{dt} = \frac{Q}{\rho V C_p} \tag{22}$$

where t [s] corresponds to time, Q [W] the added energy, ρ [kg/m^3] is the density of the material, V [m^3] to volume and C_p [J/(kg K)] is the heat capacity of the material.

1) Joule Heating: There are several ways to generate heat. In the current project the choice is made for Joule heating since this is most appropriate to fit within the design rules of the Coriolis sensor. A main limitation to the amount of heat is the risk of electro-migration. The current density is given by:

$$\phi_e = \frac{i}{A} = \sqrt{\frac{P}{\rho_\Omega l A}} \tag{23}$$

where ϕ [A/m^2] is the current density, i [A] is the current, P [W] the electric power, ρ_Ω [Ω m] the electric conductivity, l [m] the length and A [m^2] the cross-sectional area. A current density in the range of 10^9-10^{11} will form hill-locks and structural damage caused by electro-migration. The electro-migration effect is highly structure and metal dependent and measurements have to prove the threshold value of electro-migration inside the platinum heaters. For platinum specific, the electro-migration limit is about 10^{11} A/m^2. It is confirmed in literature by Srinivasan that still no electromigration occurs in thin platinum films at current density of $9 \cdot 10^{10}$ A/m^2[15]. To be on the safe side, a density of $5 \cdot 10^9$ A/m^2 is taken as a starting point.

2) TCR: The Temperature Coefficient of Resistance (TCR) is also an important feature of the design, since the temperature is measured by means of resistance variations dependant on temperature. The common equation for the TCR is often described as:

$$\frac{R - R_0}{R_0} = \alpha(T - T_0) \tag{24}$$

where R_0 [Ω]is the reference resistance at a known temperature, α [1/K] the thermal coefficient and T [K] the temperature. The TCR as given as above is a first order approximation of the real temperature dependence on resistance and therefore only valid in a limited region. Including higher order system makes the system more precise, but also more complex to define the TCR. For high range platinum temperature sensors a higher order dependency is used including the Calander and Van Druten equations in the expression[16], resulting in:

$$R = R_0 + R_0\alpha \left[T - \sigma(\frac{T}{100} - 1) \cdot \frac{T}{100} - \beta(\frac{T}{100} - 1) \cdot \frac{T}{100}^3 \right] \tag{25}$$

where β is 0 for temperatures higher than $0°C$. For pure platinum the σ value is 1.49. Since it is doubtful the platinum will be pure it is unknown what the effect will be on the σ value.

Since it is stated that the resistance is linear with temperature until 800 °C[15], the linear approximation will be used.

D. Mechanics

To prevent the tubes from breaking, the tubes are suspended in the centre of the chip. To get a stiff suspension, the suspension will consist of a piece of tube with closed ends. The approach used is a cylindrical tube, but in reality the tube is semi-cylindrical and contains the tube flats.

The main problem using a straight beam is the chance of buckling due to thermal expansion. Therefore the force of buckling is investigated. First the moment of inertia I_p of a circular tube is given, this moment of inertia is a approximation and holds when the wall thickness t is much smaller than the radius of the tuber_{tube}.

$$I_p = \pi r_{tube}^3 t \tag{26}$$

where I_p [kg/m^2] is the moment of inertia of the pipe, r_{tube} [m] is the radius of the pipe and t [m] is the thickness of the pipe. The next step is finding an equation which gives the elongation dx [m] of the tube. This elongation is dependent on the expansion rate of the material. The strain ϵ [-] be calculated when this expansion is related to the length l [m] of the beam.

$$\epsilon = \frac{2dx}{l} \tag{27}$$

Using this strain the total force due to temperature F_T [N] acting on the beam can be calculated:

$$F_T = E\epsilon(2\pi r_{tube} t) \tag{28}$$

To prevent buckling, this force may not exceed the maximum buckling force, thus:

$$F_T < F_{mech} \tag{29}$$

The buckling force F_{mech} [N] is given as[6]:

$$F_{mech} = \frac{4\pi^2 E I_p}{l^2} \tag{30}$$

Another limitation to its minimum length is the required length for active heating.

IV. Designs

In this section the overall design is discussed and the different implementations are explained. Each chip can be divided in a few sub-items. In Figure 4 the main sections are highlighted. In this figure the green represents the metallic layer and blue the area that is etched. In the Appendix all the designs are attached. There are in total 9 regular designs and 2 test designs. For each section the differences between the designs will be discussed.

A. Design limitations

Since it is aimed to combine the integrated Wobbe Index with the Coriolis technology, that technology will be used. This will also to limitations to the design. The technology consists of tubes with a diameter of approximately 40 μm. This limits the throughput of the gas. To increase the cross-sectional area multiple tubes can be put parallel. Another aspect of the tubes is the wall thickness. Due to the fabrication process the wall thickness with be about 1.8 μm. In reality the geometry is not circular, as shown in Figure 5. In the figure are flats on top of the tubes visible. On those flats are the platinum tracks with a height of 200 nm located.

In Table I the conversion values for a methane mass flow of 1 μg/s are shown. The densities used for methane and air are 0.656 and 1.257 respectively.

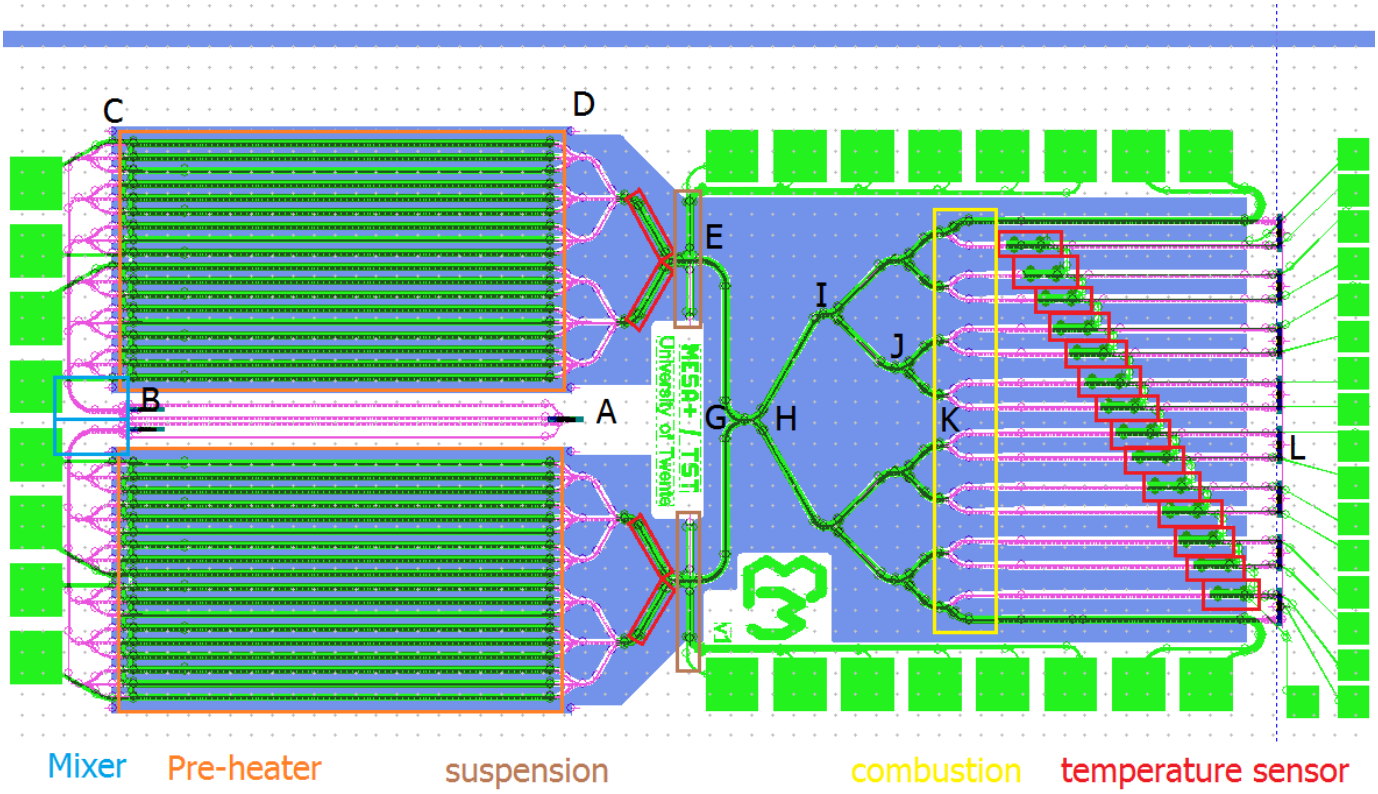

Fig. 4. Chip version 1 with the selected main sections on the chip; green is the metallic layer, blue the part that is etched

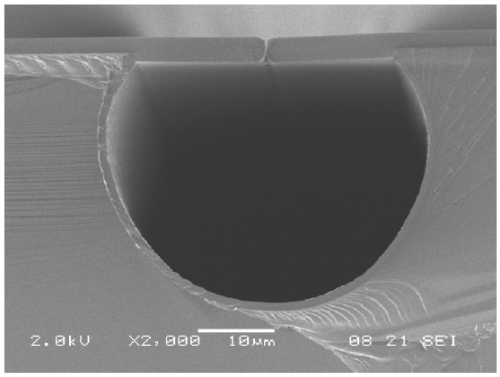

Fig. 5. Cross-section of the tube fabricated in the process

TABLE I
MASS FLOW AND VOLUME FLOW RELATIONS FOR A MASS FLOW OF METHANE OF 1μG/S

mass flow methane	1 μg/s
volume flow methane	1.52 mm^3/s
volume flow air	14.47 mm^3/s
mass flow air	17.36 μg/s
total mass flow	18.36 μg/s

B. Fluidics

First it is verified that the flow is laminar. Therefore the Reynolds number is calculated. The tube in the preheating section contains a length of 4 mm. The Reynolds number is calculated using eq.4:

$$Re = \frac{\rho \overrightarrow{v} D_h}{\mu} = 14.85 \tag{31}$$

since the flow consists of both methane and air, both flow are taken into account in the calculated. Therefore the value for $\overrightarrow{v}$ is taken to be:

$$\overrightarrow{v} = \frac{\phi_{Vair} + \phi_{VCH4}}{A} \tag{32}$$

where the velocity is based on a 1 μg/s flow methane. ϕ_V is the volume flow and their values are given in Table I. The hydraulic diameter is equal to the diameter which is 40 μm and dynamic viscosity is taken to be 16.6·10^{-6} kg/s^2. Since the Reynolds number is much lower than 2300 the gas will behave laminar.

As shown the flow is laminar, which means that eq.3 is valid and the pressure drop over the chip can be calculated using eq.3. In Table II the pressure drop for each section is calculated. The letters correspond to the letters given in Figure 4. From A to B are the tubes before the mixer, B to C is from the start of mixing until the begin of the pre-heater, etc. Point C to D correspond to the both sections of the pre-heater. Adding all the pressure drops this leads to a total pressure drop of approximately 39 mbar.

1) Mixing: To calculate the diffusion of gases the diffusion equation eq.6 together with the boundary condition given in eq.7 will be used. For diffusion three tubes are put parallel, leading to a with of 120 μm and a height of 40 μm. On both sides of the tube the fuel is applied while the air is applied

TABLE II
PRESSURE DROP OVER THE CHIP VERSION 1; THE LETTERS CORRESPOND TO THE LETTERS IN FIGURE 4

Section	D	l	ΔP [Pa]
A to B	40 μm	2250 μm	143
B to C	120 μm	3000 μm	40
C to D	40 μm	4000 μm	13
D to E	40 μm	2000 μm	400
E to G	80 μm	2250 μm	34
G to H	80 μm	200 μm	53
H to I	40 μm	1000 μm	2137
I to J	40 μm	750 μm	802
J to K	40 μm	400 μm	214
K to L	80 μm	2500 μm	41
total			3877

in the centre of the tube. This is also shown in Figure 6. The diffusion is simplified to a 1D-model by taking the diffusion along across the centre of the tube, in Figure 6 given as the grey line.

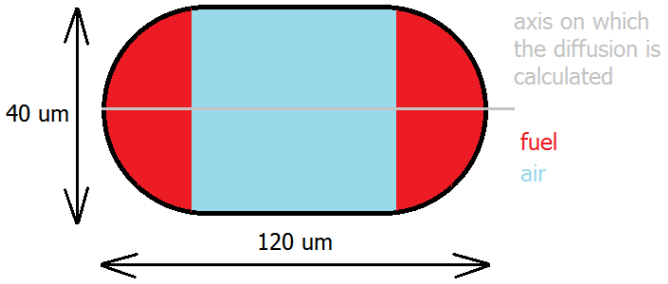

Fig. 6. Cross-section of the tube showing the initial position of the fuel and air; the grey line shows the simplified 1D model

In Figure 7 the methane density is shown across the tube after a specified amount of time. This amount of time can be converted to tube length by means of the volume flow and the cross-sectional area.

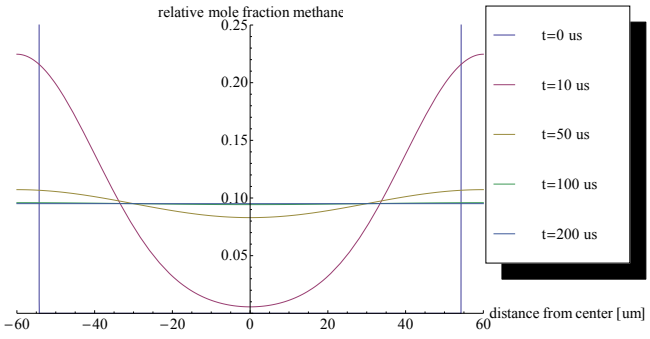

Fig. 7. methane density profile along the grey line given in Figure 6 at several time intervals

Since the required tube length is dependent on the volume flow and time, the required tube will not be dependent on the tube diameter. This is also shown in Figure 8 where the required tube length is plotted against the tube size. The sizing of the tube is done in such a way that the ratio between the height and width is kept constant. The reason that the required distance is independent on the diameter is due to the fact that a wider tube leads to a longer diffusion time. This increase in required time is counteracted by the slower flow in the tube.

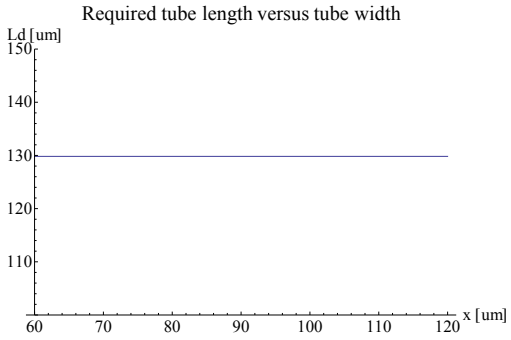

Fig. 8. Constant required tube length versus the width of the tube. The tube is scales maintaining the height:width ratio as shown in Figure 6

The mixture is sufficient mixed when the methane density is within certain limits. In the design this limit is taken within 5% of its final value, which is a volume density of 9,5%, thus the methane density must be between 9% and 10% everywhere across the tube. In Figure 9 the required tube length is shown for different volume flows.

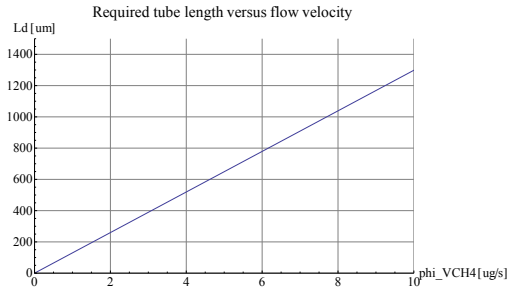

Fig. 9. Required tube length for different volume flows

In all of the designs a tube with a width of 120 μm is taken and a length of 750 μm. As shown a minimum length of 130 μm is needed for a required mixture. A much longer tube is used so that, if needed, the flow could be increased. The maximum related to the methane mass flow is shown in Figure 9 and shows that for a tube length of 750 μm a maximum methane mass flow of 5.5 μg/s can be used .

C. Pre-heating

After the gases are mixed, the gas heated to a value just below the auto-ignition point. On the chip the there are four pre-heater elements of which one is shown in Figure 10, where the length between the turns is 4 mm. On the tubes are flats located as shown in Figure 5 and the flats are bit wider than the tubes to prevent etching holes in the tube. A reasonable widths of the flats are 60 μm. Since two tracks are located on each tube, the width of the heater will be 30 μm.

This design is used on chip 1 and 6. Since this amount of voltage is quite high, on the other chips the amount of connections is doubled and the heater is split in 2 so that the required voltage is divided by 2.

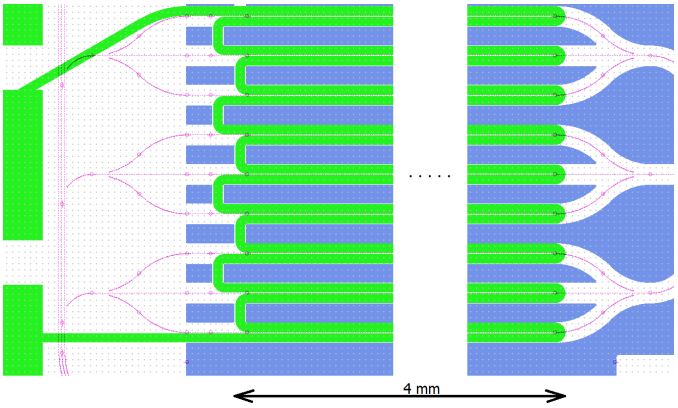

Fig. 10. Pre-heating element with a tube length of 4 mm

1) Heating simulations: The maximum temperature gained by heating the tube is simulated by means of FEM simulations. For simplicity a circular tube is taken though which the fluid flows. The tube is also used as the heat generated medium.

In Figure 11, the temperature profile in the centre of the tube is shown. In the simulation the flow is normalized to the methane flow and the methane flow is parametrized from 1 μg/s to 25 μg/s. The current density through the tracks is taken to be $5 \cdot 10^9$ A/m^2. The graph shows that the flow influences the required length of the tube.

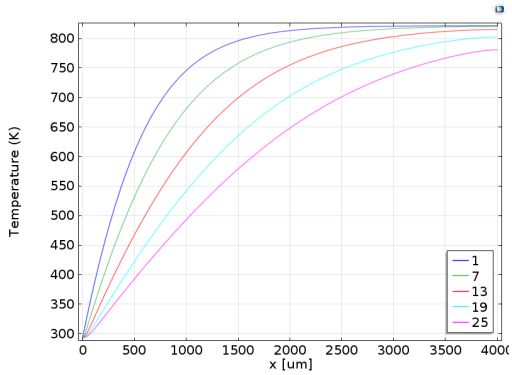

Fig. 11. FEM-simulation of the heat transfer inside a single tube for different mass flows in μg/s where the gas is evenly divided over all 36 tubes.

Also the influence of input power by means of Joule heating is investigated. In Figure 12 the relation between the maximum temperature, which is measured at the end of the 4 mm tube, and the applied current density is shown. This shows that a current density of at least $5 \cdot 10^9$ A/m^2 is needed to heat the tube to 850 K.

For each chip the amount of temperature can be tuned by means of the current density. The length of the chip limits the maximum flow to reach this temperature. For a temperature of 800 K, a maximum flow of 10 μg/s can be used.

D. Suspension

In all the designs the same suspension has been used. This suspension is shown in Figure 13. In this design the tubes are suspended directly after the pre-heating. The required length

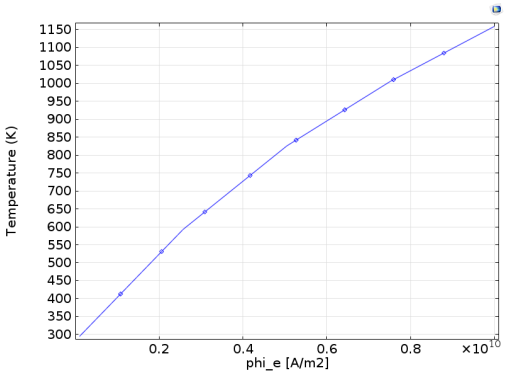

Fig. 12. Maximum reachable temperature at different current densities for a tube with two metal tracks which have both a width of 30 μm and a methane flow of 1 μg/s at the end of the 4 mm tube

of the suspension tubes is limited due to the active heating to reduce the conduction losses to the environment. To satisfy the technology the thickness of the tube is 1.8 μm and the diameter of the tube is 40 μm. The thermal conductivity of silicon nitride is taken to be 27 W/mK. As heating element a 15 μm wide and 200 nm high layer of platinum is used and the length of the heating element is twice the length of the tube, this is also shown in Figure 13. The maximum expected temperature will be around 600 °C, thus 873 K since it has to stay just below the ignition temperature. Calculating the problem using the equations eq.18 and eq.23 leads to a minimum tube length of:

$$\frac{k}{l} \cdot A\Delta T = \phi_e^2 whl\rho_\Omega \rightarrow \tag{33}$$

$$l = \sqrt{\frac{kA\Delta T}{\phi_e^2 wh\rho_\Omega}} = 475\mu m \tag{34}$$

with k =27 W/mk, $A = 2.2 \cdot 10^{-9}$ m^2, T =600 K, ϕ_e =5·10^9 A/m^2, h =200 nm, w =30 μm and ρ_Ω =105 Ωm. In the designs a length of 500 μm is used to have some extra heating.

Using the chosen length, the buckling can be investigated. First the expansion is calculated dependent on the thermal gradient of the tube. Silicon nitride has an expansion value α of 3.3·10^{-6}/K. Since there is an thermal gradient on the tube, the expansion can be calculated, by solving the following intregral:

$$\int_0^{L_{tube}} \alpha\Delta T / L_{tube} \cdot x dx \tag{35}$$

where L_{tube} is the total length of the tube, which is 500 μm. Solving the integral with ΔT=600 K leads to an expansion of 0.5 μm. Using eq.27 and eq.28 where E=200 GN/m^2 the total force due to thermal expansion is 45 mN. To gain stable expansion, this force should be smaller than the maximum buckling force. The buckling force is calculated using eq. 30:

$$F_{mech} = \frac{4\pi^2 EI_p}{l^2} = 0.413N \tag{36}$$

where E=200 GN/m^2, I_p is calculated using eq.26 and is equal to $\pi(20 \cdot 10^{-6})^3 \cdot 1.8 \cdot 10^{-6}$. The length of the tube l is

500 μm.

Since this value is much higher than the introduced force, buckling effects will not occur.

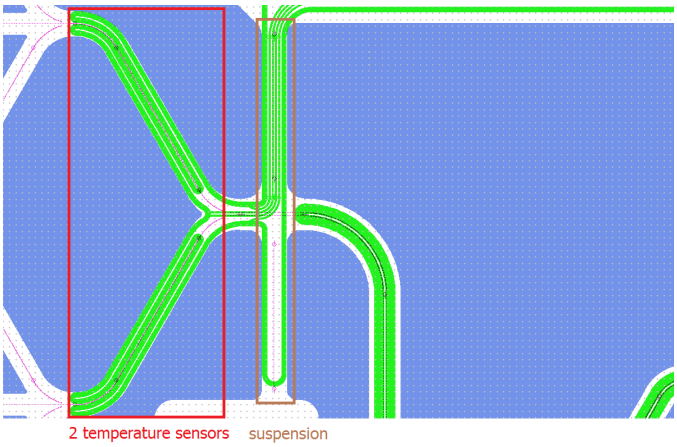

Fig. 13. 2 Temperature sensors and suspension

E. Combustion

After recombination of both parts, the tubes branch out to decrease the flow velocity in such a way that the velocity is below the flame velocity. The output flow of the flame is:

$$v = \frac{\phi_V}{A_{cs} \cdot N_{tubes}} = \frac{1.62 \cdot 10^{-8}}{2.85 \cdot 10^{-9} \cdot 16} = 0.35 m/s \qquad (37)$$

This is the final flow velocity and is used in design 1,2,3,5,7,8 and 9, and are included in the Appendix. Since the behaviour of combustion is not fully known at micro-scale, it is difficult to predict the correct flow velocity. Therefore the flow velocity is decreased in chip 4 and 6. On chip 6 the tubes are wider compared to the other tubes, resulting in a lower flow velocity. In chip 4 more tubes are drawn and every 2 tubes are connected with each other, which may lead to damages during manufacturing. In Figure 14 the combustion region of both chip version 1 and chip version 4.

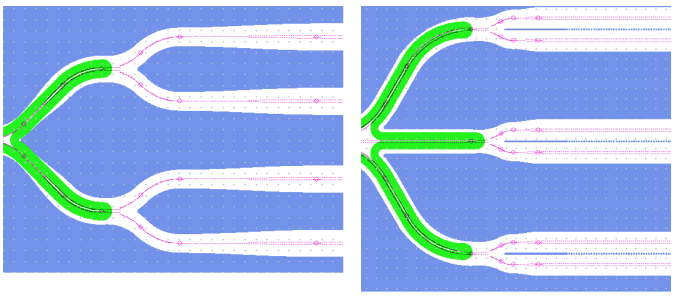

Fig. 14. left: combustion region of chip version 1; right: combustion region of chip version 4

In the designs used the flow is after preheating united to one or two places on the chip. This is done to gain locally a high flow velocity to prevent flashbacks on the input flow of methane. From this spot with the high flow velocity the net cross-sectional area increases, which is done both by widening the tube and by splitting the tube. This is done until the maximal available area is used, leading to 16 parallel tubes, except for design 4 where 24 tubes are used. The net flow velocity will be 0.35 m/s in case the flow is at 293 K and 1 bar. As already discussed in theory it is unknown what the burning velocity will be due to quenching.

On chip 5 and 8 are the combustion/exhaust tubes interconnected. In case in one tube the gas combusts and in the other tube not, this interconnection enables to transfer the flame to the other tubes.

F. Temperature sensors

To measure the resistance of the sensor a 4-point measurement will be done. Using a current source the current through the resistance will be fixed. By using the other two connections to the same resistance of purely the sensor will be measured. Due to temperature increase the resistance of the sensor will increase and will be a measure of the temperature.

The sensitivity of the sensor will highly dependent on the thermal coefficient of the material. For pure platinum this thermal coefficient is in the order of 3895$\cdot$ 10^{-6}/K, but in the device itself the platinum is contaminated by titanium. Therefore the thermal gradient is lowered to approximately 2500$\cdot$ 10^{-6}/K.

Since the current is kept at a constant value, the variation of the resistance will be directly related to the voltage. The maximum sensitivity is mainly dependent on the current since a higher current means a higher voltage. On the other hand it must be realized that an higher current induces more heat and thus self-heating will also induce some errors.

In the designs two different sensors are drawn, the first sensor is placed directly after pre-heating and shown in Figure 13 and it main goal is to measure the temperature of the fluid due to preheating. The second sensor is placed on the tubes to monitor the temperature due to combustion and is shown in Figure 15. In version 1,2,3,6 and 7 the sensor is placed with varying positions regarding the combustion as shown in Figure 16 to measure the temperature profile along the tubes. For the pre-heat temperature sensor the current can also be used for active heating. Therefore the current through the elements will be in the order of a maximum of 15 mA. The resistance of the element itself will be approximately 120 Ω. At this current level a sensitivity of 4.5 mV/K can be achieved.

In the sensor to measure the combustion no heating is required. Therefore the current through the wire kept low, so no heating is induced on the tubes. Again, first the expected resistance is calculated, leading to a value of approximately 210 Ω. For this sensor using those values a sensitivity of 0.5 mV is achieved in case a current of 1 mA is used. The sensitivity scales proportional with current thus higher sensitivity can be achieved. On the other hand also the error translating the voltage to temperature must be taken into account which might contain much larger errors than due to the sensitivity.

G. Test chips

Beside the discussed chips, also one design has been made to test the temperature increase over the distance heated on

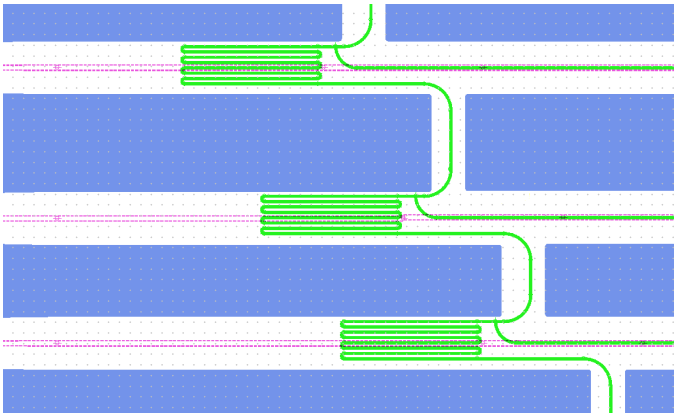

Fig. 15. 3 sensors to measure the temperature on each tube

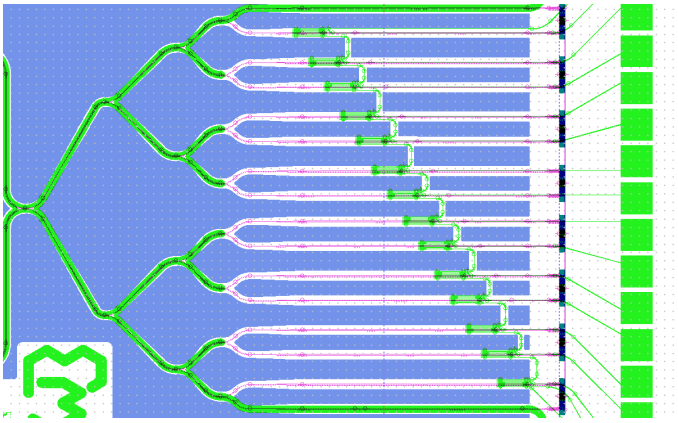

Fig. 16. Output tubes with sensing element on each tube with varying positions in to measure the temperature profile along the tubes

the chip. The other design the main purpose is for illustration, since the aim is to burn to gas through a certain text.

1) Test-structure 1: Test-structure 1 is generated to gain insight in heating the gas. Instead of heating the gas in tubes with a length of 4 mm, lengths ranging from 500 μm to 5000 μm with an increment of 500 μm are used. For each length three parallel tubes are used. After the heating element a sensor of 500 μm is used to measure the average temperature. In Figure 17 an example of such a test-structure is shown.

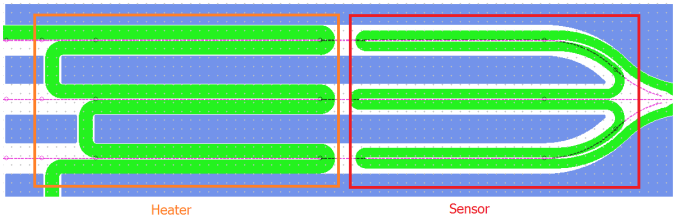

Fig. 17. Heating element of 500 μm and sensor element as a test structure

After this test-structure the gas is heated even further so that, if possible, an attempt can be made to combust the gas. The gas exits the system due to an hole in the tube; if combustion occurs the flame will stabilize on the edges of this hole.

2) Test-structure 2: The second test-structure is made mainly for illustrative purposes when combustion can occur. The combustion will take place when the gas exits the system through the text ”Mesa+ TST University of Twente”.

H. Other designs

There are also designs that were thought of, but were not fabricated. Instead of first mixing and than heating, the gas could also be heated and than mixed. Since the gas is first heated, the tube is hot for a long distance, resulting in loss of heat. The gas is also travelling faster, but also the diffusion constant will increase, leading to similar lengths required for mixing.

Another design thought of, was to make a system containing separate tube wherein the combustion occurs. This design did not come through since non-ignition may occur.

Instead of methane, also hydrogen could be tested. Hydrogen has a much higher speed velocity (about 3m/s), thus more gas can be transported. The drawback is that hydrogen weights less, thus harder to measure. The advantage is that hydrogen flames between 4 and 75 volume percent and its optimum is at 29.5 volume percent. The ignition temperature is about 845 K, about 60 K lower than methane. Since propane has a lower auto-ignition value, propane could also be a good substitute to test wit. Propylene is also a good alternative; it requires a lower ignition temperature and is more easily heated up. Regarding flow control is propylene easier to measure than methane.

Another manner to decrease the required temperature is by means of applying a catalyst. Platinum is a common catalyst for methane combustion. To apply a catalyst further research is needed on the chemical reaction and integration in the fabrication.

I. Assembly design

The chip explained above is connected to a piece of aluminium. The chosen material is aluminium due to its high conductivity. In this aluminium piece, three holes are drilled for the fluid. On top of the aluminium base the chip and PCB are glued. The drilled holes are large enough to put the fluid tube in it. The final result is shown in Figure 18, where the chip is positioned within the PCB.

V. Fabrication process

The sensor is fabricated using the Coriolis fabricating process. Figure 19 shows a summary of the fabrication process.

The process starts with a doped <100> p++ wafer on which a 500 nm thick low stress silicon nitride layer is deposited. Then the fluidic inlets and outlets are etched from the backside of the wafer. The etching stops at the silicon nitride layer and therefore has the by monitored carefully(Figure 19a). Then a 1 μm thick layer of TEOS oxide is deposited on the back side of the wafer. Using a chromium patterned mask the wafer is patterned which forms the outline of the channel. Using reactive ion etching the pattern is transferred to the silicon nitride layer. Next, the TEOS layer and chromium mask are removed and another silicon nitride layer is grown with a

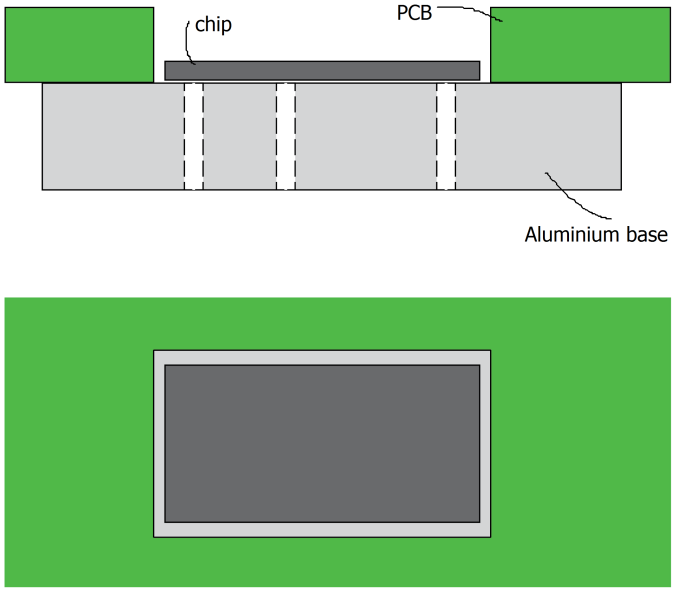

Fig. 18. Design of the chip package

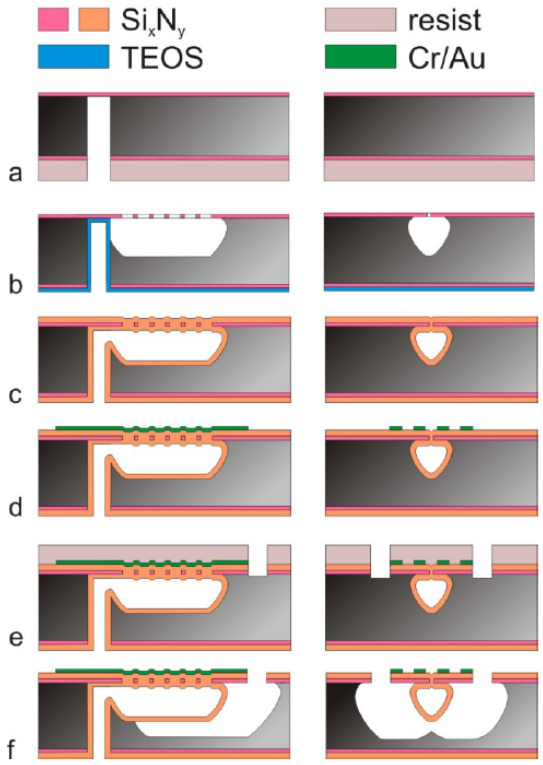

Fig. 19. Outline of the fabrication process; left column: cross-section along the length of the tube; right column: cross-section perpendicular to the tube[5]. Cr/Au is replaced by Ti/Pt

thickness of 1.8 μm, sealing the channel wall and etch holes in one single step(Figure 19c). Then a 10/200 nm layer of titanium and platinum is sputtered and patterned(Figure 19d). This step creates the heaters and the temperature sensors on the tube. After metal patterning the release windows are opened by means of reactive ion etching. The structure is released released by an isotropic silicon plasma etch step followed by resist removal step. The resulting structure can be seen in Figure 20.

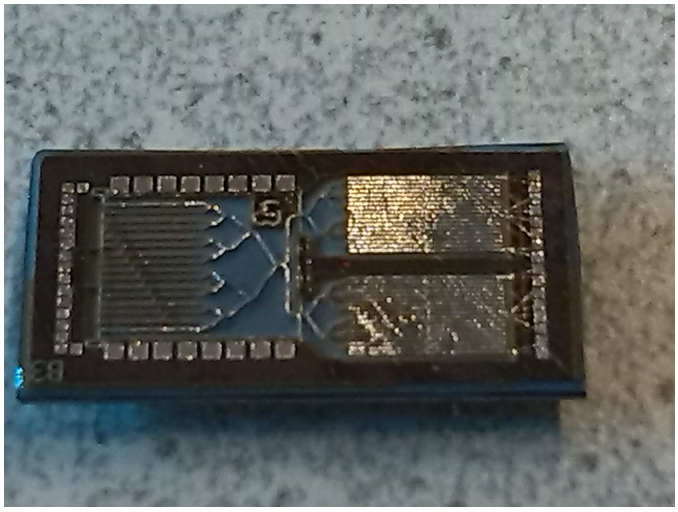

Fig. 20. Photograph of the complete sensor chip version 7

A. *Resulting chip*

The chips retrieved after micro-machining contain traces of photoresist. This is visible in Figure 21. Here the platinum layer in the figure coloured white is deposited nicely. On the layer beneath it there is contamination of photoresist. In Figure 22 it is visible that there is also photoresist beneath the platinum. This could have influence on the temperature since an extra layer is added.

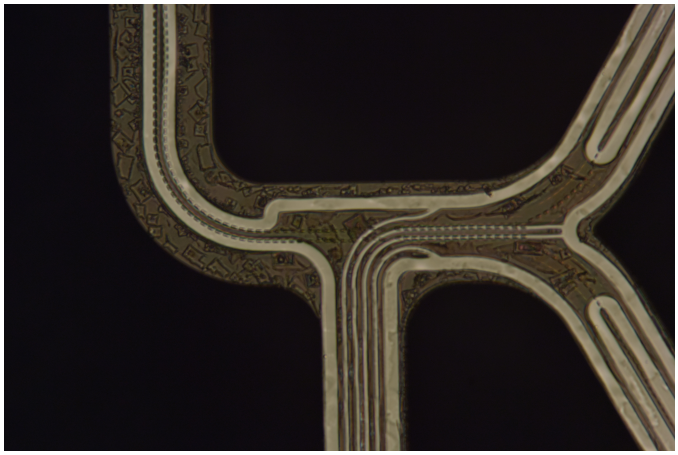

Fig. 21. Section of a chip showing the residue next to the metallic(white) tracks

Also the platinum layer itself shows delamination. In Figure 23 delamination in the platinum layer also shown. It is not clear if delamination consists of accumulation of platinum particles or that also here other material is beneath it. Also in Figure 24 is delamination in the platinum layer shown. Here the platinum shows itself to be much smaller than the expected. By measuring the resistance of the wire, a comparable value is measured with regards to a normal wire. One explanation

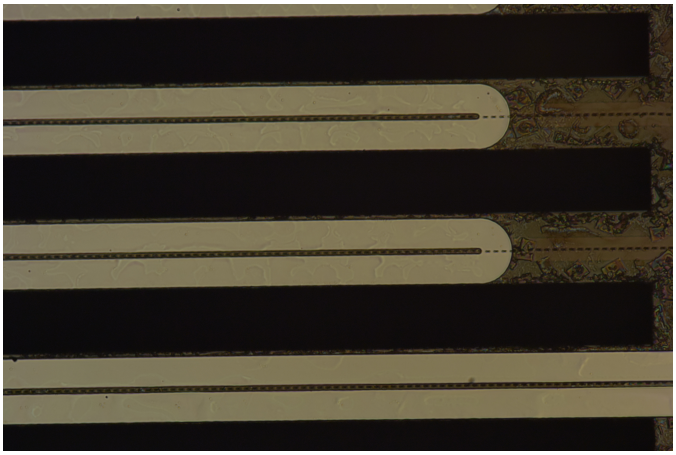

Fig. 22. Nicely deposited metallic tracks with residue underneath

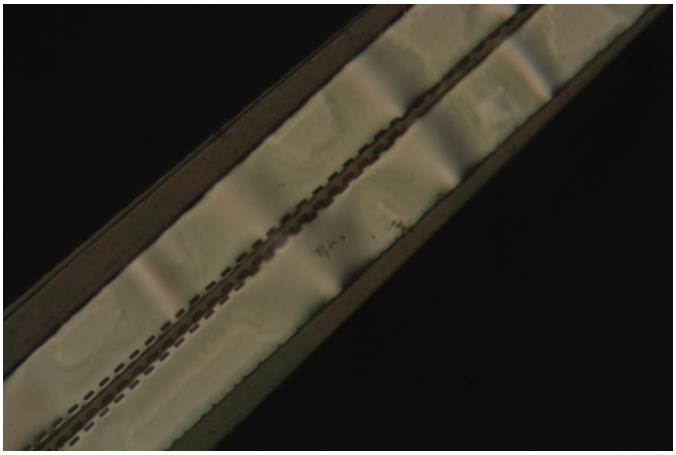

Fig. 23. Delamination in the platinum tracks

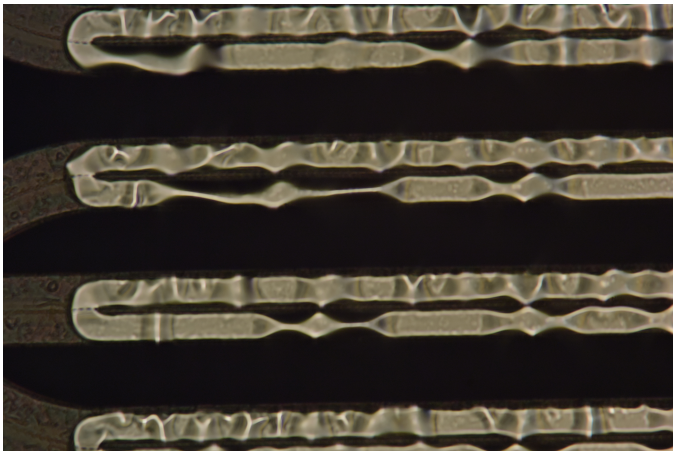

Fig. 24. Extreme delamination and twisting in the metallic layer.

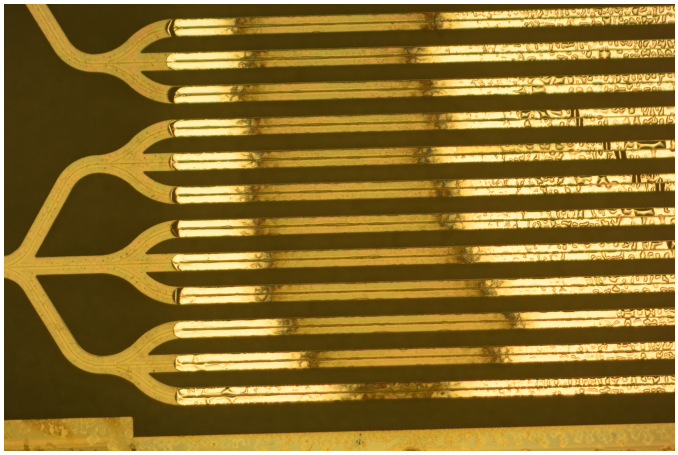

Fig. 25. Platinum partly removed from the tubes

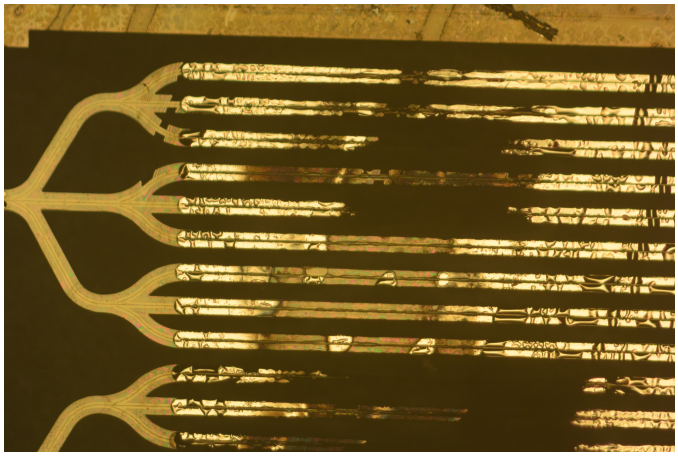

Fig. 26. Parts of the tubes are lost in the process

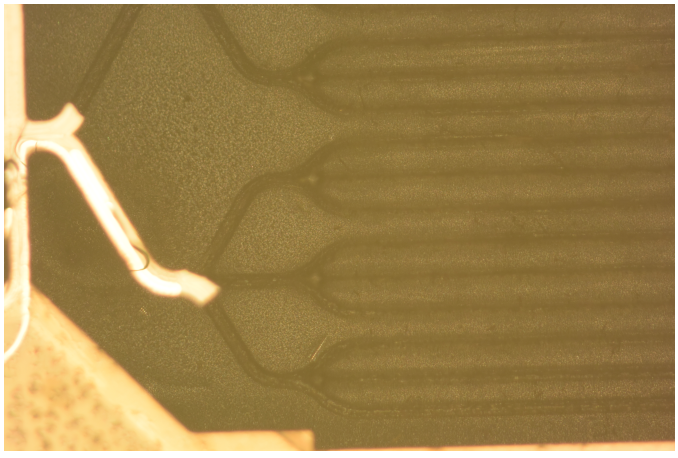

Fig. 27. On some chips all the tubes were removed, only the relief at the bottom remains

is that the wire is also here delaminated and also twisted, and thus the reflection is different.

A lot of chips show a partial removal of the platinum layer. An example is shown in Figure 25 where the platinum top layer is fully removed. several chip lost tubes, be it partial or fully. This is shown Figure 26 and Figure 27.

B. Post-fabrication

After fabrication the first step is annealing the chips. Since the adhesion layer of platinum is titanium a trade-off must be made between resistance drop, degradation of thin film and required temperature. Since the chip should be able to measure 600 °C, the annealing temperature must be at least higher. The

first chip are heated up to 650 °C using a 10 °C/min step and annealed for 1 hour since then the combustion temperature can be reached but also the thin film stays intact as much as possible. Before and after annealing the resistance is measured. Before annealing the resistance as 1.14 $k\Omega$ and after annealing 0.94 $k\Omega$. For the given temperature this resistance drop is in line with other experimental results in literature[17].

The next step is gluing. This is done as given in section IV-I. The result is shown in Figure 28.

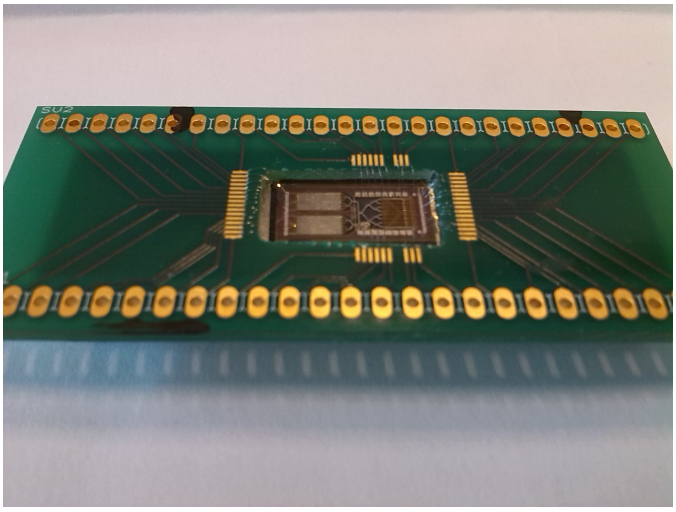

Fig. 28. Fully assembled chip version 5

The gluing needs to be sealing the chip, therefore the following attempts have been made. For the first chips the aluminium piece has been lubricated with glue, attempting to make a nice mono-layer of glue. Since this attempt failed since gas leaked form underneath the chip. Therefore an another approach is used to obtain a nice mono-layer of glue with a high coverage. First a piece of cloth is lubricated with glue. Since the glue draws in the cloth, a fully lubricated area can be obtained. Next, the aluminium is stamped on the glue and enough is sticking to the aluminium to add the chip.

VI. Measurements

In this section the measurements on the chips are done. For each measurement the protocol and setup and results are discussed.

A. TCR measurement

After fabrication the chips, the TCR dependency of the resistors is measured. To measure the TCR correctly the temperature needs to be stable. Therefore the following protocol has been established: each and every second the temperature of the oven is measured. This temperature will be a measure to heat the oven even further or to keep te temperature constant. When the temperature is within certain boundaries, for the measurements ± 0.5 K, and for a certain amount of measurements, for the measurements taken to be 1000, the temperature and resistance of the resistors are measured. The resistors are measured using a HP 34970A switching unit enabling to measure all resistors. A schematic design of the setup is shown in Figure 29.

The measurement is done for multiple temperatures ranging from 40 °C to 70 °C for each chip. From those temperatures the TCR can be retrieved by calculating α using eq.24. This measurement is performed on multiple chips. The TCR for each chip is given in Table III. On some chips there were defect resistors, the amount of resistors excluded from the average is shown in also shown in Table III. The resistance over a total of 20 resistors is calculated. Between the chips there is a difference in TCR. This could be influenced by the annealing of the chips; during annealing the properties are influenced and the result differs for annealing session. Therefore also the resistance leads to different TCR values. On the chip itself the error between the resistors is very small. The error is within 5% which is quite high, which results in large errors especially at higher temperatures. A better approximation will be obtained when the TCR of the resistor itself will be used instead of the average value.

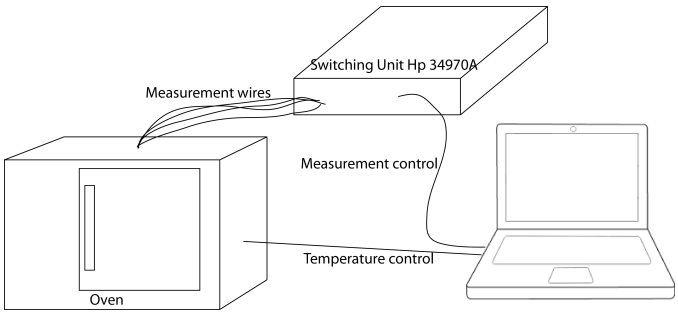

Fig. 29. Setup to measure the TCR of the temperature sensors on the chip

TABLE III
TCR measurements done for 4 different chip, showing the average TCR of the chip and the maximum error

Chip type	average TCR (10^{-6}/K)	maximum error	defect resistors
version 9	2855	<3.7%	5
version 4	2513	<1.4%	7
version 6	2512	<3.8%	2
version 4	2658	<4.8%	5

Since the chip is fully assembled dynamics of the chip can be observed. This will be done with and without gas. First the resistance due to static heating is investigated. Next, the chip dynamics is verified using nitrogen gas since then no combustions occurs and no alternation of gas composition influences the chip.

B. Heater tests without flow

Now the TCR of the chip is known temperature dependent measurements can be performed. The next measurement will be done without flow and is done by heating up the tubes locally.

To do so the temperature sensors after preheating will be used, as shown in Figure 13. To measure the temperature the current through the sensor is increased stepwise. Due to the current the temperature is increased as given in Figure 12.

For each measurement the resistance is measured when the resistance is stable.

In Figure 30 the resistance is plotted over the current through the sensor and clearly the resistance increases. It is also clear that there is a temperature rise due to the increased applied current. For the resistance the adjacent temperatures are calculated using eq. 24 and the average TCR of the chip which is α=2512·10^{-6}/K. Using the calculated temperatures it shows that temperatures of 800 °C can be achieved. To verify that the chip really reaches those temperatures a Hartmann&Braun pyrometer is used. Using this pyrometer the radiation colour is compared. From this comparison it can be estimated that the temperature is in the range between 700 and 900 °C. This is in accordance with the calculations.

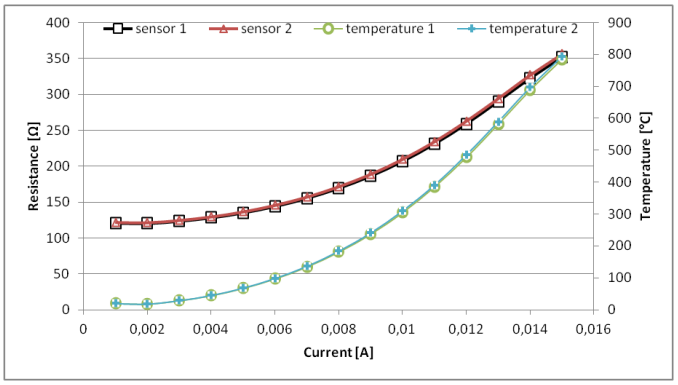

Fig. 30. Measured values of resistance and the adjacent temperatures of the sensors.

C. Test with nitrogen flow

Before methane and air is used for combustion, first nitrogen will be applied for safety. To contain all the flow inside the tube, the chip needs to be hermetically sealed. To verify the sealant, two flow-meters are used; one flow-meter on the input which is calibrated for air and one flow-meter on the output connector which is calibrated for methane. The setup is also given in Figure 31. The measurement is performed as follows: The valve of the second flowmeter is opened fully. In this case it can measure the maximum flow going through the valve. Then the flow is controlled using the first flow meter. The maximum flow applicable is the maximum flow range of both sensors.

Since the flow meters are not calibrated for the same gas, the gas is first directly applied to the second flow meter, so the second flow meter can be calibrated. Then the input flow is varied while the output valve is fully open. Measurements are performed on chip version 6 and the measurement is shown in Figure 32.

In this graph the output controller measures only a fraction of the total gas put in the chip. This means only a fraction of the fluid goes through the chip, but most of the fluid is exiting somewhere between the two flow-controllers. The leaks are quite small since the pressure drop is small enough to contain enough pressure on the output to measure flow.

Since it can be measured that a small volume of gas is travelling through the tube, measurements have been done to

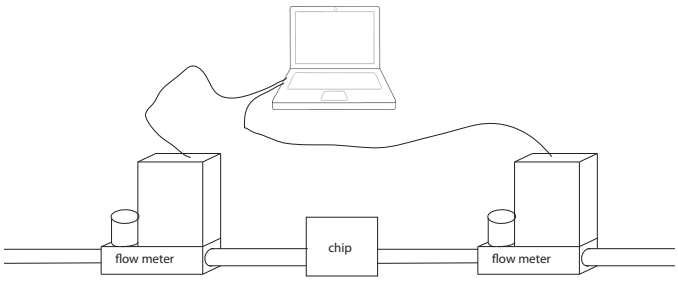

Fig. 31. Setup to measure the relation between the input gas and output gas to verify the chip is not leaking

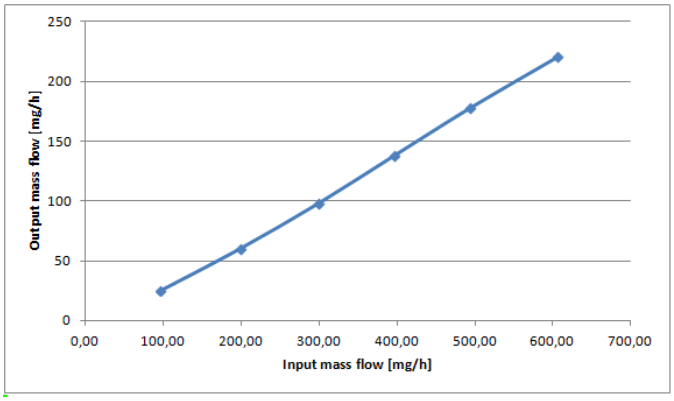

Fig. 32. Results of measuring the input flow and output flow on chip version 6

prove that this flow can be heated. To prove this influence the measurement is performed as following: First the flow applied to the chip, Next, current is applied to the heaters so that the temperature of the tubes increases. Due to the flow the tubes and the temperature sensors will also increase in temperature. When the flow is removed or lowered the effect of the flow is lowered thus the temperature will also decrease.

The measurement is performed as described above and the result is shown in Figure 34. In Figure 33 are the location and numbering of the 4 sensors and 2 heaters shown. On the

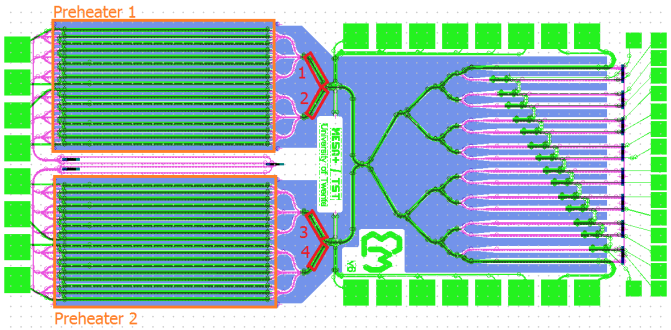

Fig. 33. Location and numbering of the 4 sensors and 2 heaters on chip version 6

chip preheater 2 in front of sensor 3 and 4 is heated. From measurement point 325 there is a rise is resistance voltage of sensor 3 and 4. The voltage increases from 0.118 V to 0.138 V which corresponds to 66.9 °C.

When the flow is removed partially, a voltage drop is observed. The voltage drops to a similar level as sensor 1 and sensor 2 and shows that total chip is heated up. Then the flow is increased and no increase of voltage can be observed. This means there is no direct relation between the measured voltage and flow velocity and therefore no conclusions can be drawn about the temperature of the flow. It seems that the measured temperature is mainly of general heating of the chip. A reason that no flow is observed could be that the gas is heated and therefore more easily can escape the chip through the small holes.

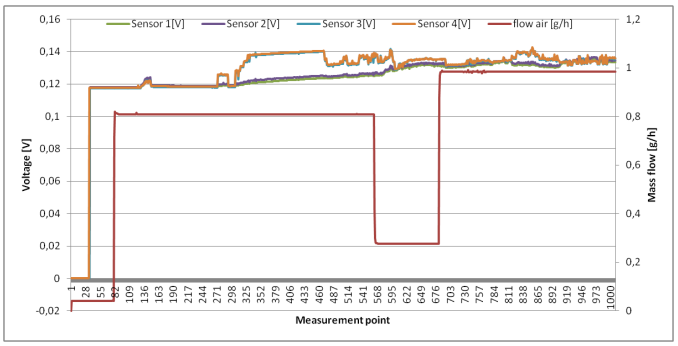

Fig. 34. Response of the temperature due to varying the mass flow while increasing the current of the heaters.

D. Tests with methane and air

Since no satisfying results regards the heating of gas can be measured no attempts have been made to burn the methane.

VII. Discussion

To design an integrated Wobbe Index Meter several disciplines are investigated. It has been shown that the mixing of the gas easily can be realized on the chip by means of diffusion. Regarding the combustion there is still uncertainty about the needed combustion velocity since the pre-heating increases the burning velocity while the small tube diameter induces quenching lowering the maximum burning velocity. To obtain the required temperature, a lot of energy is needed. To increase the maximum temperature the amount of energy per tube should be increased.

To obtain stable combustion the burning velocity needs te match the flow velocity. Since the temperature of the gas is elevated to 800 K the burning velocity will be 1.8 m/s. The burning velocity is decreases due to quenching, but the effect on the burning velocity is difficult to predict since no experiments are performed for such small tube. Future experiments are needed to gain insight in quenching.

During fabrication a titanium adhesion layer is used for attaching the platinum to the silicon nitride. The temperature performance of the platinum layer will be increased when a tantalum layer is used as adhesion layer since a tantalum layer has much better characteristics at high temperatures, compared to a titanium adhesion layer. Also higher temperatures can be reached since no deterioration of material happens below 850 °C in case of tantalum adhesion layer. Another manner to increase the performance of the platinum layer is by decreasing the required temperature. The required temperature can be lowered when the combustion is accelerated using a catalyst.

The resistance-temperature dependence shows a nice linear relation that is in line with the expectations. Using this relation a good estimation of the local temperature can be achieved. Further investigation on the TCR for higher temperatures is needed to calibrate the temperature sensor at elevated temperatures.

The chips does not show a flow dependency between the heater temperature and the temperature sensor. When the heaters are actuated a slow increase in resistance at the sensors can be measured. Since this is below 70 °C this temperature indicates the temperature of the chip itself. More investigation is needed what exactly causes the leakage on the chip. It is expected there are small holes on the tube and when the gas is heated the leakage will be increased.

VIII. Conclusion

In this report an attempt is made to obtain a microburner for Wobbe Index measurements. This basic principle consists of Coriolis flow sensors to measure the gas, a mixer to mix the fuel with air and a heater to heat the gas until auto-ignition occurs. After combustion the gas will be exhausted. The Wobbe Index will be retrieved by temperature increase at the combustion chamber.

To obtain a stable combustion research has been done on mixing, heating the gas inside silicon nitride tubes and the flow velocity required for stable combustion. Taking a starting position of a mass flow of 1 μg/s a length of 130 μm is needed for sufficient mixing. Also the heat transfer for different mass flows is investigated, resulting in a tube length of at least 3 mm for heating the gas to the correct temperature. It is also shown that the temperature is dependent on the current density through the heaters, which needs to be at least 5 GA/m^2 to heat the temperature to 850 K.

From those requirements 11 designs are made using a process to fabricate silicon tubes. On top of the tubes are platinum tracks located. During fabrication some of the tubes on the chips were destroyed. On other chips the platinum was partially removed or the platinum layer was delaminated from the tube.

On the working chips measurements have been done. The temperature dependence of the resistance show results between $2512{\cdot}10^{-6}$/K and $2855{\cdot}10^{-6}$/K between the chips. On the chip itself the difference between the TCR is below 4.8%. Also the flow through the tube is verified. The measurement shows a drop in flow, concluding the chip is leaking. Measurements heating the gas and tubes results in a increase of temperature below 70 °C and is independent of the gas flow, which is thus mainly a result of heating the chip itself.

Since there is no temperature of the gas, no stable combustion could be performed.

References

[1] A. Mouris, “Optimized fired heater control,” *Hydrocarbon Processing*, 2010.

[2] P.Ulbig and D. Hoburg, "Determination of the calorific value of natural gas by different methods," *Thermochimica Acta*, vol. 382, 2000.
[3] M. Pap, "Wobbe meter," Master's thesis, University Twente, 2011.
[4] D. J. Lötters, D. T. Lammerink, M. Pap, I. R. Sanders, M. de Boer, A. Mouris, and D. R. Wiegerink, "Integrated micro wobbe index meter towards on-chip energy content measurement," in *IEEE 26th International Conference on Micro Electro Mechanical Systems, MEMS 2013*. Taipei, Taiwan: IEEE Robotics and Automation Society, 2013, pp. 965–968. [Online]. Available: http://doc.utwente.nl/83633/
[5] J. Groenestijn, J. Haneveld, T. Lammerink, J. Lotters, M. Dijkstra, and R. Wiegerink, "Optimization of a micro coriolis mass flow sensor using lorentz force actuation," *Sensors and Actuators A: Physical*, vol. 186, 2012.
[6] M. Elwenspoek and R.Wiegerink, *Mechanical Microsensors*. Springer, 2001.
[7] R. Tilley, *Understanding Solids*. Wiley, 2013.
[8] M. Cowie and H. Watts, "Diffusion of methane and chloromethanes in air," *Canadian Journal of Chemistry*, vol. 49, no. 74, pp. 74–77, 1970.
[9] C. Rallis and A. Garforth, "The determination of laminar burning velocity," *Prog. Energy Combust. Sci.*, vol. 6, pp. 303–329, 1980.
[10] S. Liao, D. M. Jiang, and Q. Cheng, "Determination of laminar burning velocities for natural gas," *Fuel*, vol. 83, pp. 1247–1250, 2004.
[11] R. Yetter, N. Glumac, and I. Glassman, *Combustion*. Academic Press, 2014.
[12] A. factory mutual fire insurance companies, "Properties of flamable liquids, gases and solids."
[13] C. Robinson and D. Smith, "the autoignition temperature of methane," *Journal of hazardous materials*, vol. 8, 1984.
[14] Aug. 2015. [Online]. Available: http://microfarm1.rssing.com/chan-13729555/latest.php
[15] R. Srinivasan, "Microfabricated reactors for partial oxidation reactions," Master's thesis, Indian Institute of Technology, 1998.
[16] Acromag, "Criteria for temperature sesors election of t/c and rtd sensor types," 2011.
[17] D. Resnik, D.Vrtacnic, M. Mozek, B. Pecar, and S. Amon, "Experimental study of heat-treated thin film ti/pt heater and temperature sensor properties on a si microfluidic platform," *J. Micromech. Microeng*, vol. 21, no. 2, p. 025025, 2011.

IX. Acknowledgements

In performing the assignment I would like to show my gratitude to Prof. dr. ir. J.C. Lotters and Dr. ir. R.J. Wiegerink for giving good guideline for the assignment during the consultations. I thank Ir. D. Alveringh for his daily guidance and R.P.G. Sanders for his assistance on the measurement set-ups.

Appendix
Designs of the chips

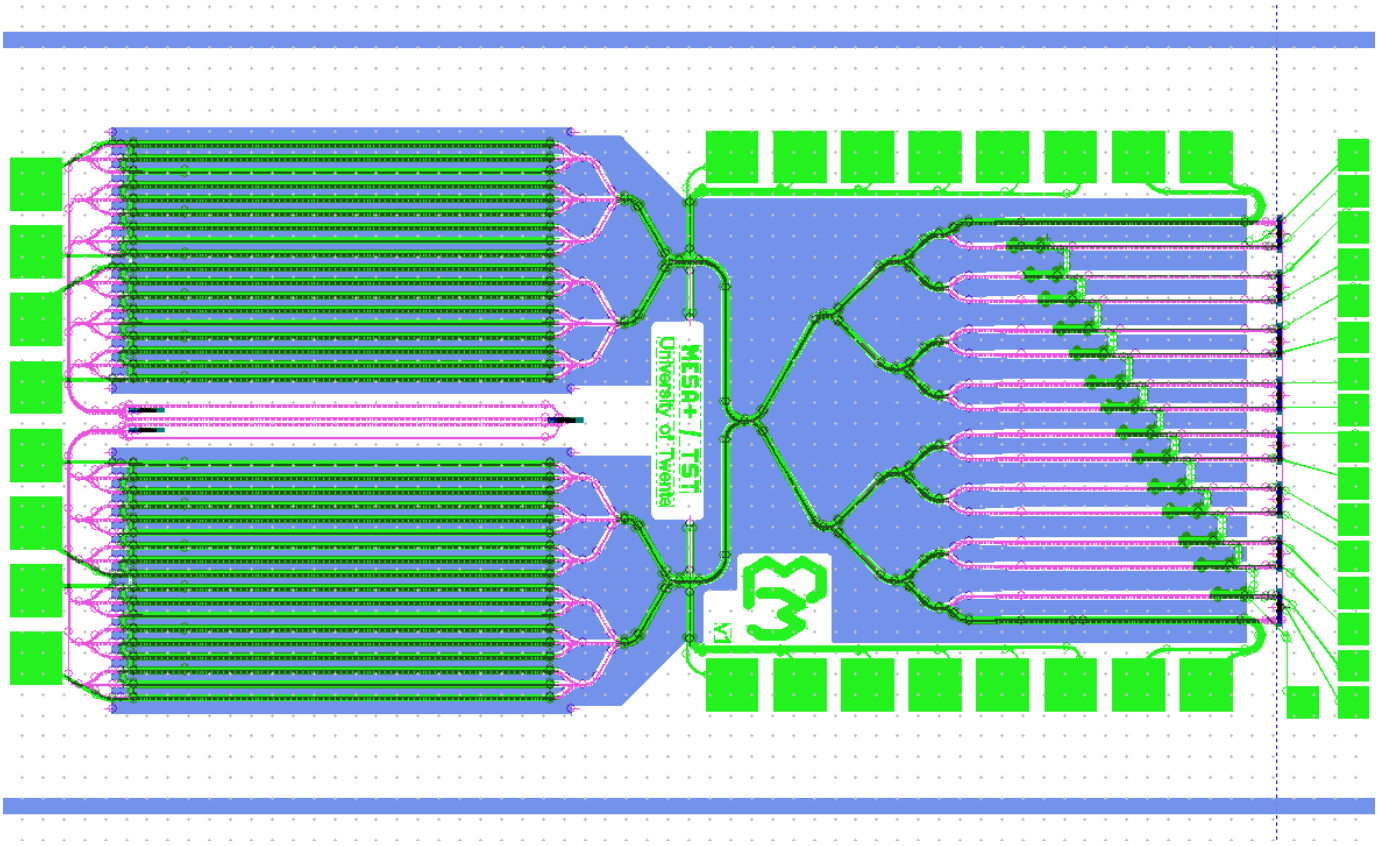

Fig. 35. chip version 1

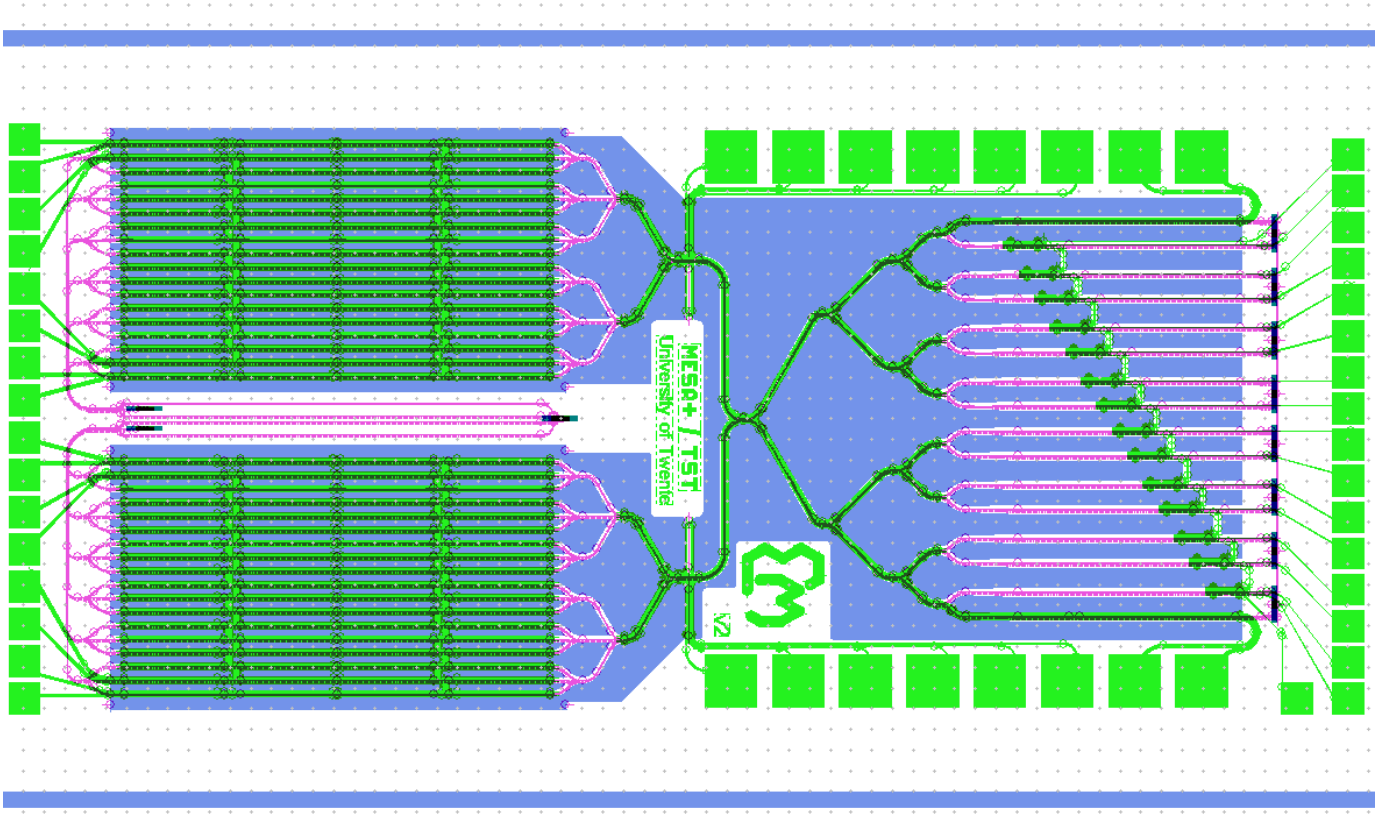

Fig. 36. chip version 2; number of heaters is increased compared to chip 1

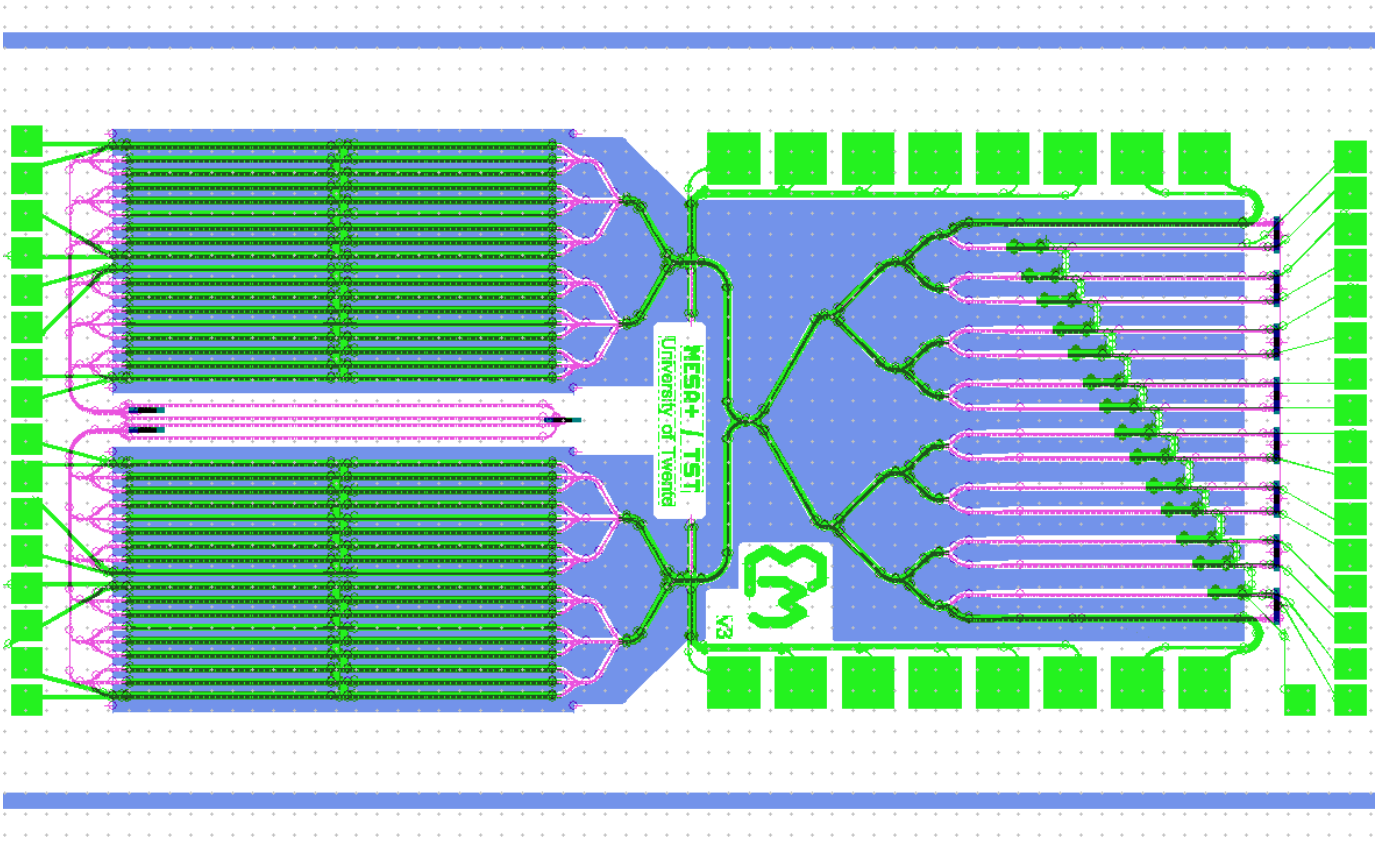

Fig. 37. chip version 3; number of heaters is increased compared to chip version 1, another variation than chip 2

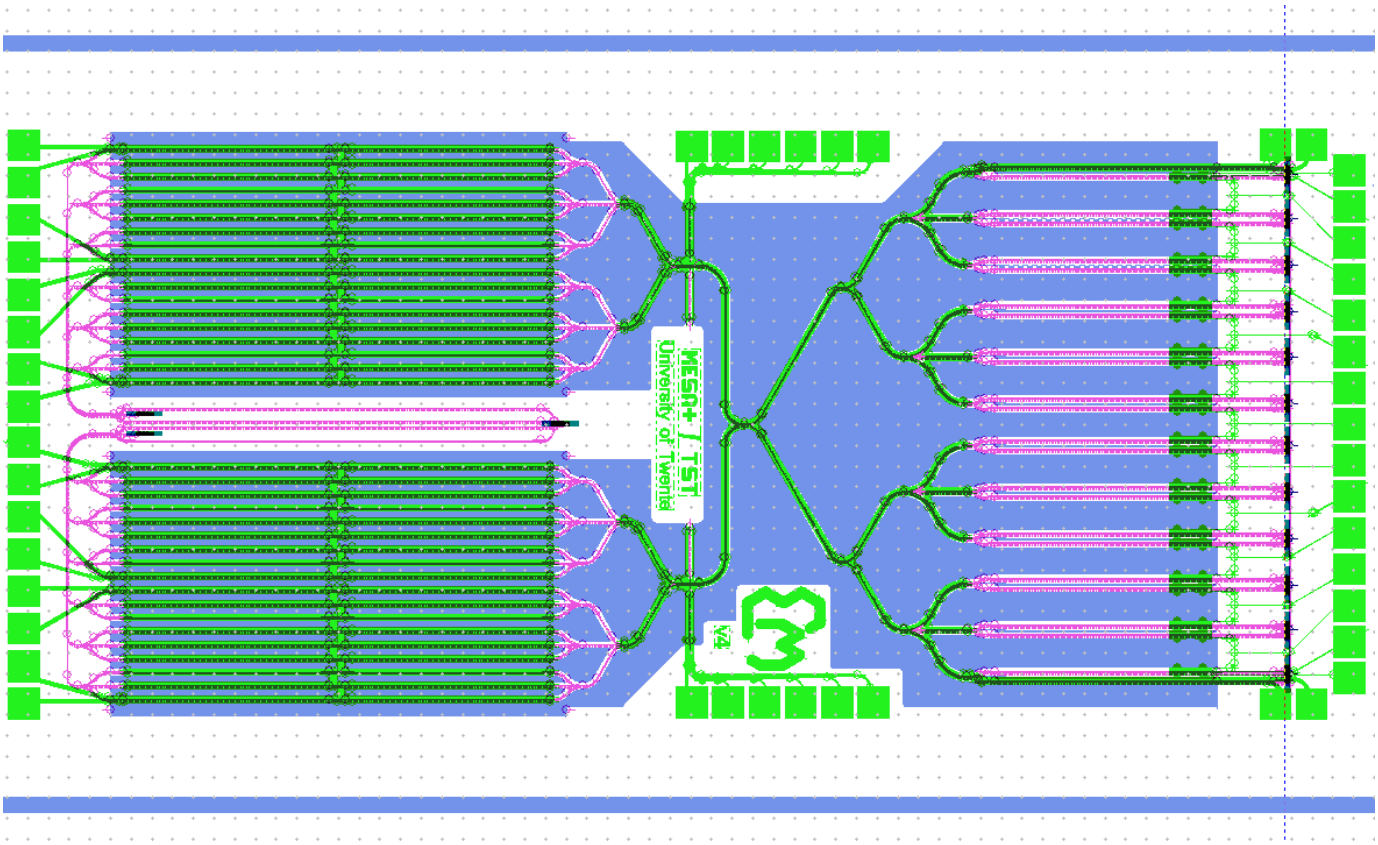

Fig. 38. chip version 4; more exhaust tubes than chip version 3, the output temperature sensors are put on equal distance after combustion

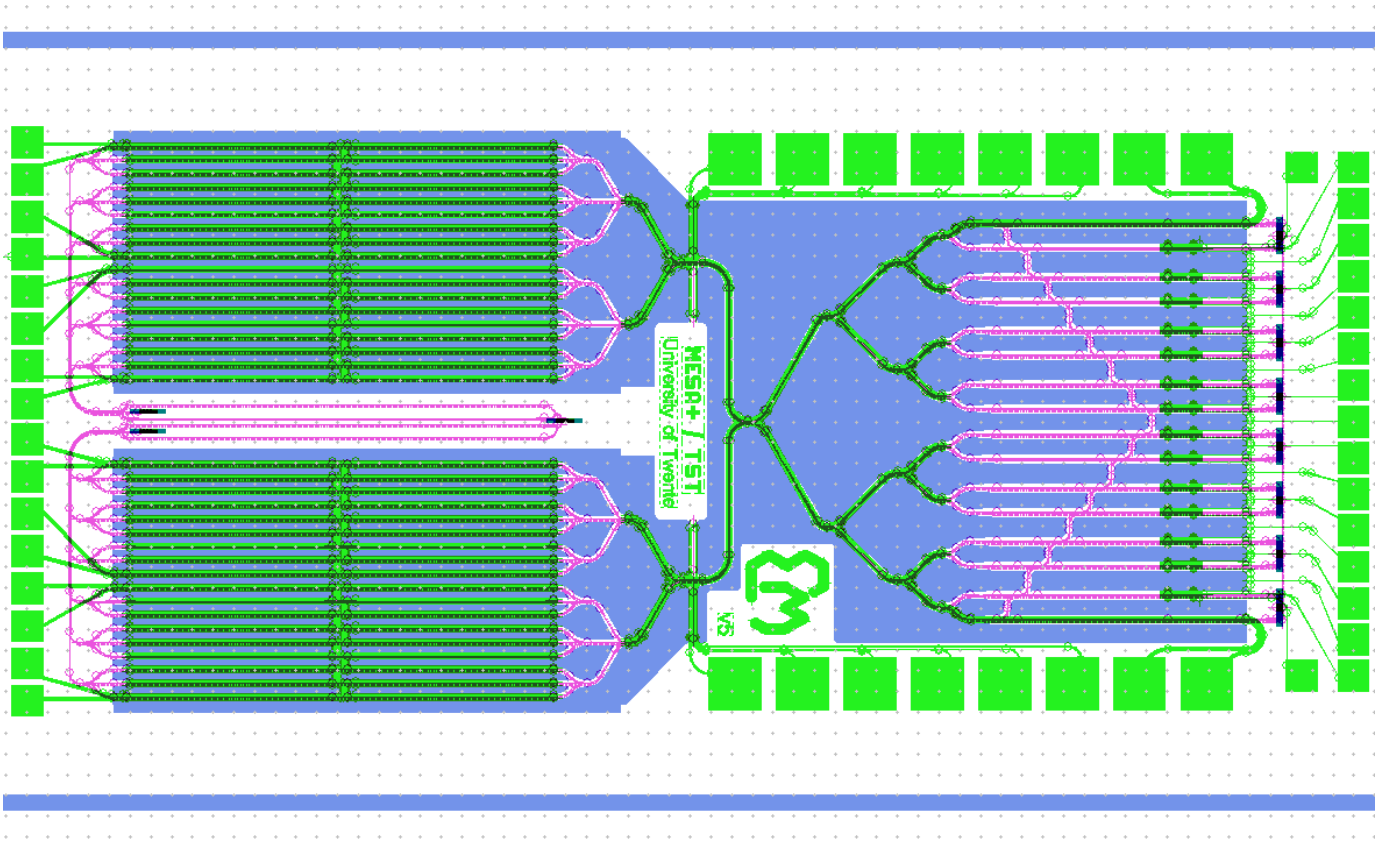

Fig. 39. chip version 5; exhaust tubes are interconnected, the output temperature sensors are put on equal distance after combustion

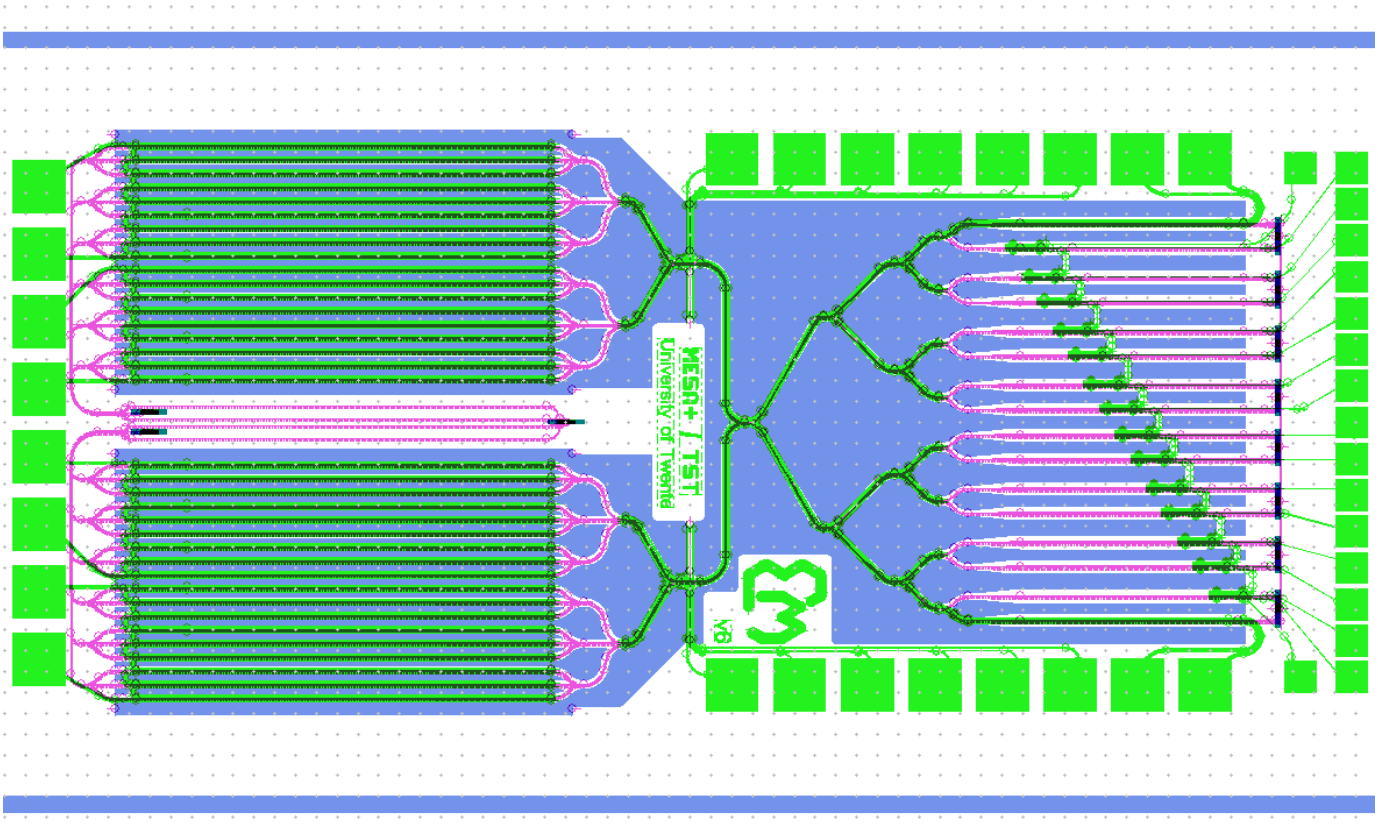

Fig. 40. chip version 6; all tubes are wider than chip 3

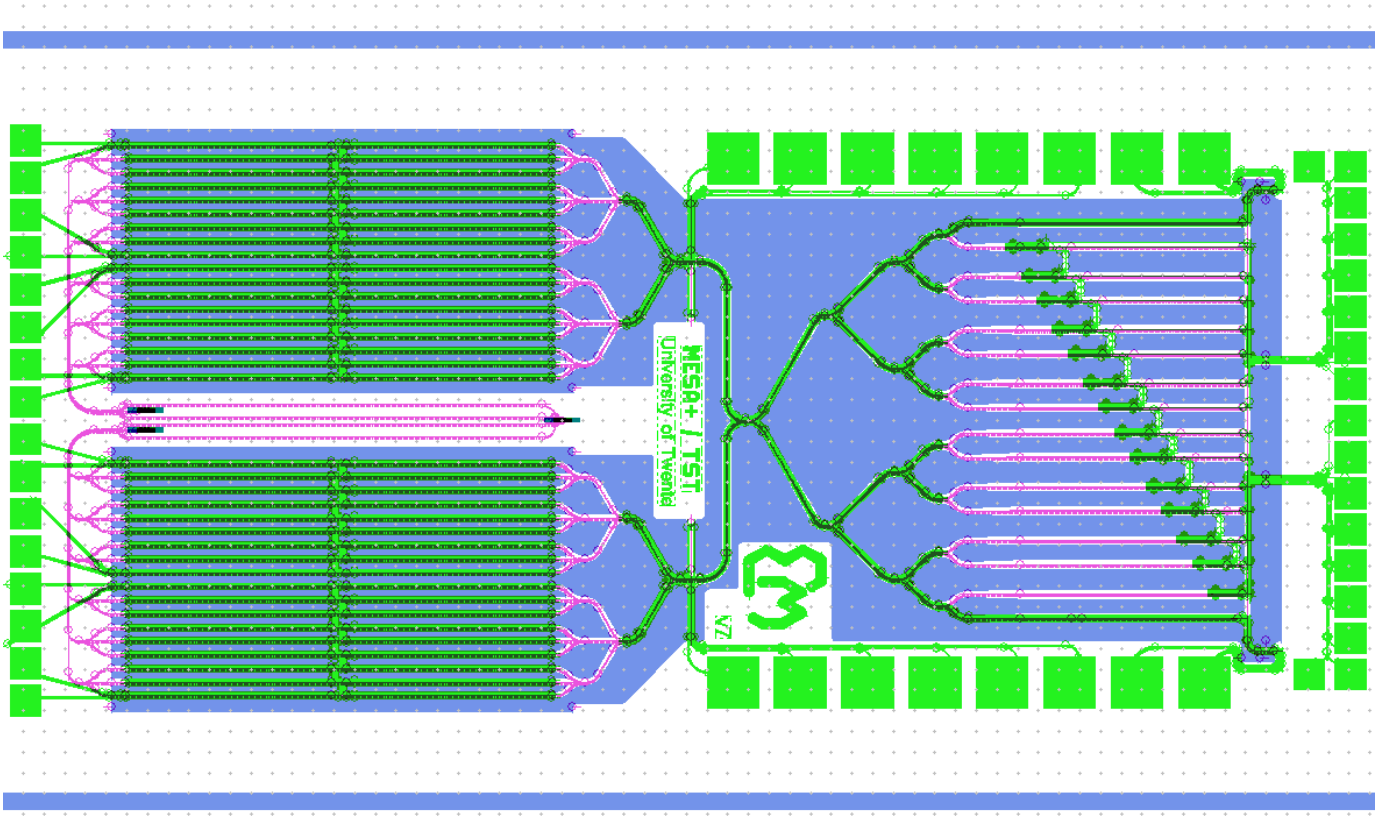

Fig. 41. chip version 7; exhaust is directly connected to the environment

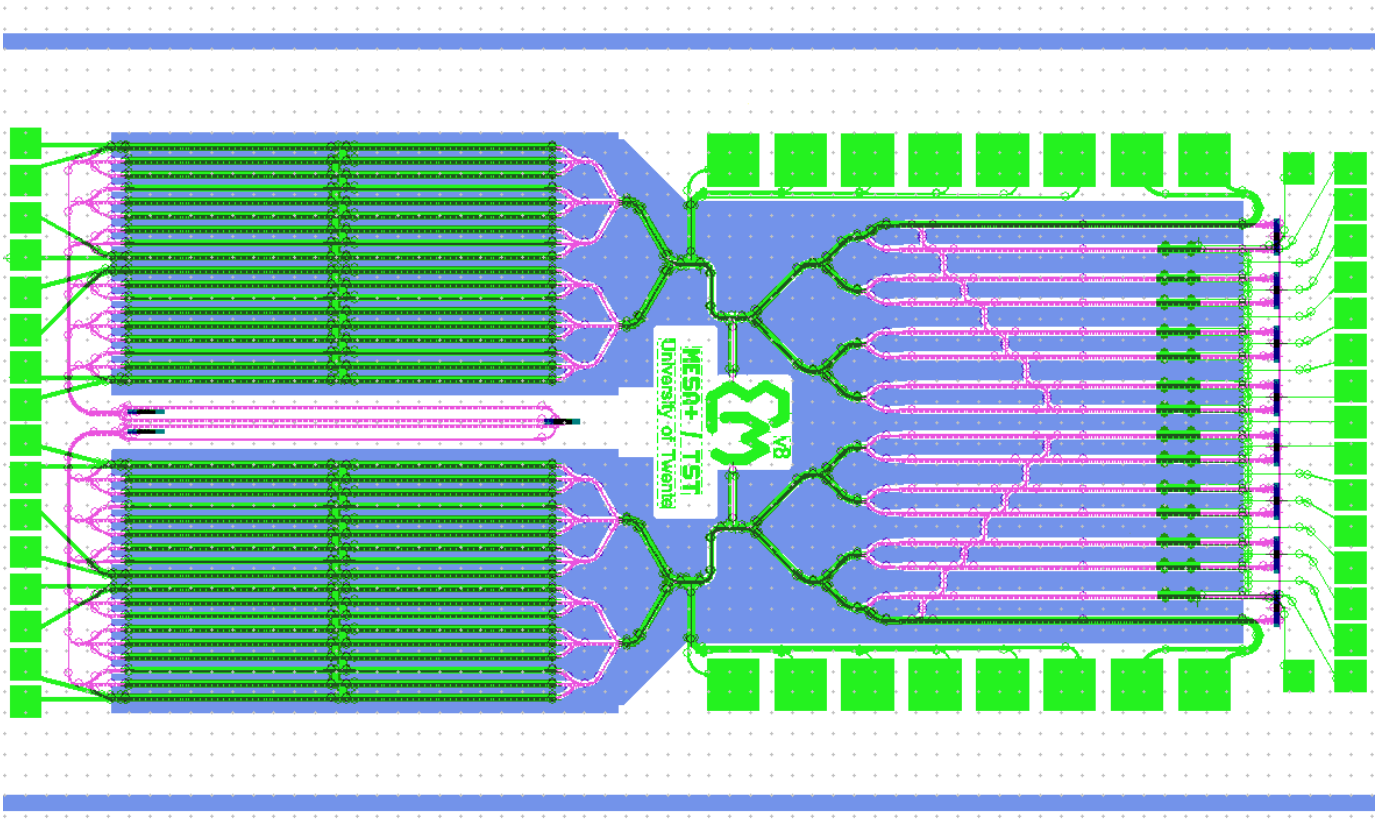

Fig. 42. chip version 8; chip is divided into two parts, no combination occurs

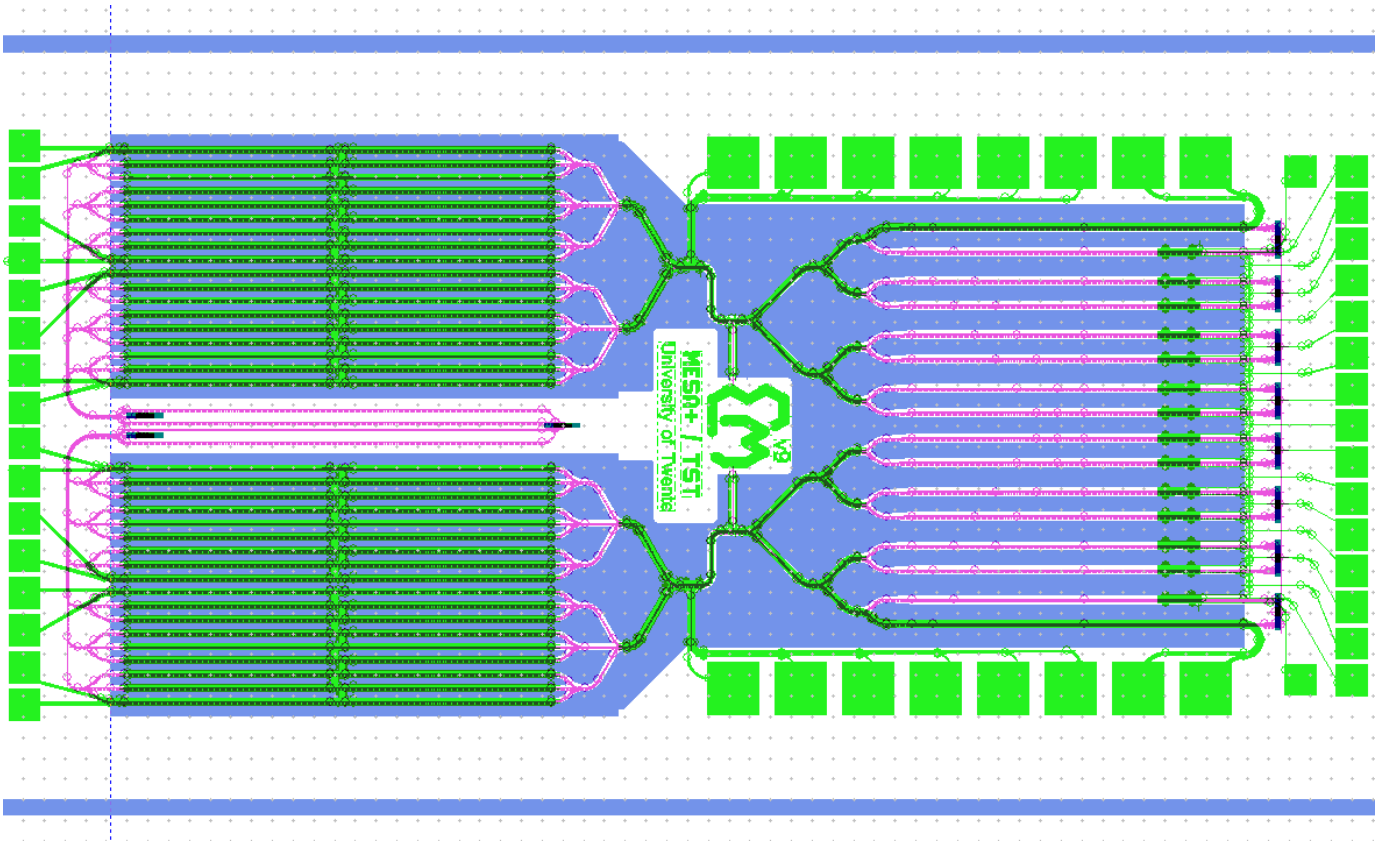

Fig. 43. chip version 9; similar to chip version 8, except the output sensors are put on equal distance to combustion

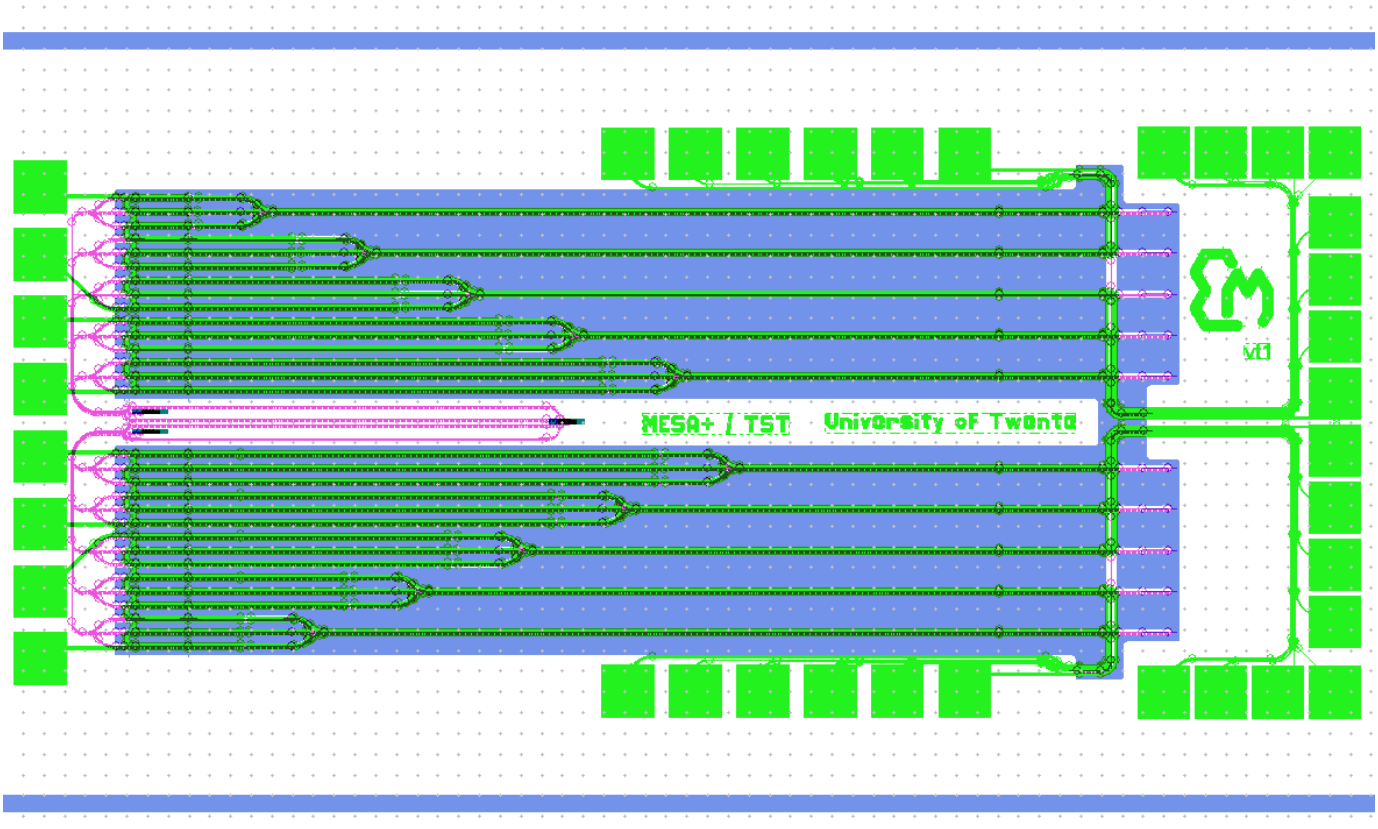

Fig. 44. chip version t1

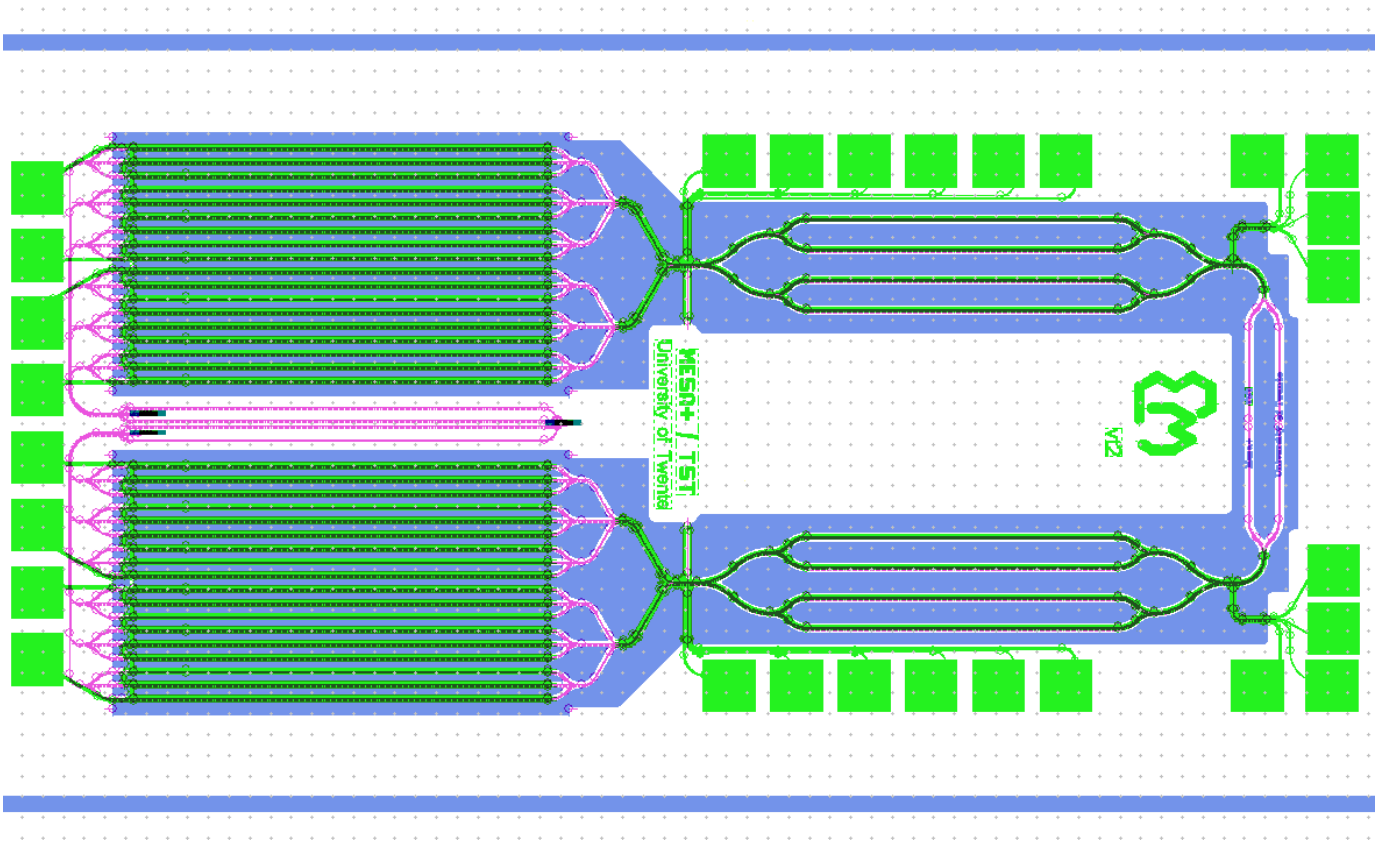

Fig. 45. chip version t2